

AD-A221 756

WRDC-TR-89-4119

SELF-LUBRICATING-DIAMOND-LIKE COATINGS DEPOSITION

James Hirvonen
Ward Halverson

SPIRE CORPORATION
PATRIOTS PARK
BEDFORD, MA 01730



DECEMBER 1989

Final Report for Period 20 November 1986 - 28 March 1989

APPROVED FOR PUBLIC RELEASE; DISTRIBUTION IS UNLIMITED.

MATERIALS LABORATORY
WRIGHT RESEARCH AND DEVELOPMENT CENTER
AIR FORCE SYSTEMS COMMAND
WRIGHT-PATTERSON AIR FORCE BASE, OH 45433-6533

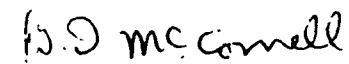
771C
1990
8

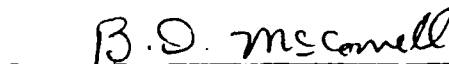
NOTICE

When Government drawings, specifications, or other data are used for any purpose other than in connection with a definitely Government-related procurement, the United States Government incurs no responsibility or any obligation whatsoever. The fact that the government may have formulated or in any way supplied the said drawings, specifications, or other data, is not to be regarded by implication, or otherwise in any manner construed, as licensing the holder, or any other person or corporation; or as conveying any rights or permission to manufacture, use, or sell any patented invention that may in any way be related thereto.

This report is releasable to the National Technical Information Service (NTIS). At NTIS, it will be available to the general public, including foreign nations.

This technical report has been reviewed and is approved for publication.


B.D. McCONNELL, Project Manager


B. D. McCONNELL, Chief
Nonstructural Materials Branch

FOR THE COMMANDER


MERRILL L. MINGES, Director
Nonmetallic Materials Division

If your address has changed, if you wish to be removed from our mailing list, or if the addressee is no longer employed by your organization please notify WRDC/MLBT, WPAFB, OH 45433-6533 to help us maintain a current mailing list.

Copies of this report should not be returned unless return is required by security considerations, contractual obligations, or notice on a specific document.

UNCLASSIFIED

SECURITY CLASSIFICATION OF THIS PAGE

REPORT DOCUMENTATION PAGE				Form Approved OMB No. 0704-0188	
1a. REPORT SECURITY CLASSIFICATION Unclassified			1b. RESTRICTIVE MARKINGS		
2a. SECURITY CLASSIFICATION AUTHORITY			3. DISTRIBUTION/AVAILABILITY OF REPORT Approved public release distribution is unlimited		
2b. DECLASSIFICATION/DOWNGRADING SCHEDULE					
4. PERFORMING ORGANIZATION REPORT NUMBER(S) FR-10102			5. MONITORING ORGANIZATION REPORT NUMBER(S) WRDC-TR-89-4119		
6a. NAME OF PERFORMING ORGANIZATION Spire Corporation		6b. OFFICE SYMBOL (if applicable)	7a. NAME OF MONITORING ORGANIZATION Wright Research and Development Center Materials Laboratory (WRDC/MLBT)		
6c. ADDRESS (City, State, and ZIP Code) Patriots Park Bedford, MA 01730			7b. ADDRESS (City, State, and ZIP Code) Wright-Patterson AFB OH 45433-6533		
8a. NAME OF FUNDING/SPONSORING ORGANIZATION		8b. OFFICE SYMBOL (if applicable)	9. PROCUREMENT INSTRUMENT IDENTIFICATION NUMBER F33615-87-C-5203		
8c. ADDRESS (City, State, and ZIP Code)			10. SOURCE OF FUNDING NUMBERS		
			PROGRAM ELEMENT NO. 6 5502F	PROJECT NO. 3005	TASK NO. 51
					WORK UNIT ACCESSION NO. 18
11. TITLE (Include Security Classification) Self-Lubricating Diamond-Like Coatings Deposition					
12. PERSONAL AUTHOR(S) Dr. James Hirvonen, Dr. Ward Halverson					
13a. TYPE OF REPORT Final		13b. TIME COVERED FROM 86-11-20 TO 89-3-28		14. DATE OF REPORT (Year, Month, Day) December 1989	
15. PAGE COUNT 52					
16. SUPPLEMENTARY NOTATION					
17. COSATI CODES			18. SUBJECT TERMS (Continue on reverse if necessary and identify by block number)		
FIELD	GROUP	SUB-GROUP	ion beam diamond-like wear, hexagonal		
			deposition hardness adhesion, lubricious,		
			boron nitride friction, cubic dense		
19. ABSTRACT (Continue on reverse if necessary and identify by block number)					
<p>Ion beam enhanced deposition (IBED) has been used to deposit hard, adherent thin films of boron nitride with a significant cubic crystal structure present. A number of analytical techniques have been used to characterize these coatings including X-ray photoelectron spectroscopy (XPS); X-ray diffraction (XRD); transmission electron microscopy (TEM); Raman spectroscopy; nuclear radiation analysis (NRA); Rutherford Backscattering spectroscopy (RBS); and IR spectroscopy. Friction and wear behavior of these coatings was also conducted. The IBED-i-BN thin films generally exhibit a high microhardness ($K_{HN} = 2000-3000$, i.e. 20-30 GPa) and good adhesion to the silicon and 304 stainless steel substrates. All films (except one) had the hyperstoichiometric boron concentration. The ratio $[B]/[N]$ approached the theoretical value at the highest current densities of the nitrogen beam. Many of the i-BN coatings exhibited low friction (~ 0.1) against 440°C stainless steel and Si_3N_4 counterfaces. Friction seems to increase with increasing B/N ratios.</p> <p style="text-align: right;">(continues)</p>					
20. DISTRIBUTION/AVAILABILITY OF ABSTRACT <input type="checkbox"/> UNCLASSIFIED/UNLIMITED <input type="checkbox"/> SAME AS RPT. <input checked="" type="checkbox"/> DTIC USERS			21. ABSTRACT SECURITY CLASSIFICATION Unclassified		
22a. NAME OF RESPONSIBLE INDIVIDUAL Bobby D. McConnell			22b. TELEPHONE (Include Area Code) (513) 255-9033		22c. OFFICE SYMBOL WRDC/MLBT

19: ABSTRACT (Continued)

There is a strong demand for diamond-like coatings of boron nitride (BN) in a large number of tribological applications including cryogenic bearings and adiabatic engines. Commercial use of BN coatings has previously been impeded by sample to sample reproducibility problems which have been overcome by the innovative Spire process using ion beam enhanced deposition (IBED).

The results of the Phase I research were extremely encouraging, producing coatings with Knoop hardnesses greater than 2500 Kg/mm^2 and dimensionless wear coefficients approaching 10^{-7} . Spire Corporation proposes to expand both the scope and extent of Phase I research to obtain the optimum process parameters which will be used for commercial scale-up. These will include ion dose, ion energy, deposition rate, ambient gas background, local temperature, and layer thickness. In addition to these IBED will be evaluated for its ability to deposit commercially viable diamond-like BN coatings and the best coating parameters will be identified. The Phase I data have indicated that the full potential of "diamond-like" BN coatings may be demonstrated as commercially feasible in the short term.

Accession For	
NTIS CMA&I	<input checked="" type="checkbox"/>
DTIC TAB	<input checked="" type="checkbox"/>
Unannounced	<input type="checkbox"/>
Justification	
By	
Distribution/	
Availability Codes	
Dist	Special
A-1	



SUMMARY

During the past year, Spire Corporation has extensively expanded its study of thin films of boron nitride produced by the ion beam enhanced deposition (IBED) method. The broadening of this investigation beyond the Phase I and first year efforts has been aided by improvements to the IBED facility as well as by the availability and use of a wider variety of analytical techniques to characterize these coatings.

In conjunction with other projects within Spire's Thin Film Technologies Lab and with support from various government and private sector funding, the IBED facility has been overhauled and improved. Among the major improvements are the installation of a new, larger capacity, electron beam evaporator; dual ion beam neutralizer filaments; a new grid system for the ion source; and mounting jigs and hardware for rotating (planetary-type) depositions. All of these modifications have been undertaken to help improve the uniformity and reproducibility of the IBED depositions as well as increase the system throughput.

The number of different analytical techniques used to characterize the coatings has been expanded to include the following: X-ray photoelectron spectroscopy (XPS or ESCA), X-ray diffraction (XRD), transmission electron microscopy (TEM), Raman spectroscopy, and nuclear reaction analysis (NRA) in addition to the Rutherford backscattering spectroscopy (RBS) and IR spectroscopy analyses performed earlier in the program. We have also completed a more extensive analysis of the friction and wear behavior of these coatings.

Although the complexities of the boron nitride system, and the subtleties of its cubic phase formation are not completely understood, we feel that we have now identified a reproducible approach to producing hard, adherent, thin films of IBED boron nitride with significant cubic phase present.

TABLE OF CONTENTS

Section	Page
1 INTRODUCTION.	1-1
2 BACKGROUND	2-1
2.1 Ion Beam Enhanced Deposition (IBED)	2-1
2.2 Application to Nitride Films	2-2
2.3 Previous i-BN Studies	2-2
3 PHASE II EXPERIMENTAL PROGRAM	3-1
3.1 Spire's I-BN Study	3-3
3.1.1 Thermal Stability	3-3
3.1.2 Chemical Stability	3-6
4 EXPANDED ANALYSIS OF i-BN COATINGS	4-1
4.1 Nuclear Reaction Analysis (NRA)	4-2
4.1.1 Results and Discussions	4-3
4.1.2 Conclusions	4-7
4.2 Auger and XPS Analysis	4-7
4.3 Structure and Crystallinity	4-10
4.4 Infrared and Raman Spectra Analysis	4-14
4.5 Friction and Wear Behavior.	4-18
5 POSSIBLE i-BN APPLICATIONS	5-1
5.1 Optical	5-1
5.2 Low-Z Coating	5-1
6 ACKNOWLEDGEMENTS	6-1
REFERENCES.	REF-1

LIST OF ILLUSTRATIONS

<u>Figure</u>		<u>Page</u>
1-1	Schematic Diagram of the IBED Process	1-3
2-1	Depiction of Events Including Displacement Spikes Occurring During Ion Bombardment of a Surface	2-3
2-2	Calculated Thermal Spike Temperature Following Ion Bombardment	2-3
3-1	Schematic of Spire's Ion Beam Enhanced (or Assisted) Deposition (IBED) System (a) and Depiction of Process (b) Combining Electron Beam Evaporation (Boron) with Simultaneous Ion (Nitrogen) Bombardment	3-1
3-2	Microhardness Variation with B/N.	3-4
3-3	Moh's #9 (Al_2O_3) Scratch Adhesion Test Across Silicon (left) BN (right) Boundary (10 g load)	3-5
3-4	RBS Spectra of Unannealed and Annealed BN Thin films (approximately 2000 angstroms) on Silicon Substrate	3-5
4-1	Nitrogen and Boron Distributions in the Sample #1103	4-3
4-2	Nitrogen and Boron Distributions in the Sample #0626	4-3
4-3	FRES Spectra of the Samples #0626 and #0121	4-4
4-4	Deuterium Induced Particle Spectra of the Samples #0626 and #0121	4-5
4-5	The Dependence of the [B]/[N] Ratio on the Deposition Parameters	4-6
4-6a	AES Data for G.E. CBN Reference Sample	4-8
4-6b	AES Data for i-BN Coating (1500 angstroms sputtered).	4-8
4-6c	AES Data for i-BN Coating (2500 angstroms sputtered).	4-8
4-7	XPS Depth Profile of IBED i-BN Coating.	4-9
4-8	Three-Dimensional Montage of Boron (1s) Binding Energy Peak as a Function of Depth in IBED i-BN.	4-9
4-9	Core Electron Excitation Region (a) and Plasmon Loss Region (b) for IBED i-BN Coating.	4-11

LIST OF ILLUSTRATIONS (Concluded)

Figure		Page
4-10	Core Electron Excitation Region (a) and Plasmon Loss Region (b) for Hexagonal BN Standard	4-11
4-11	Diffraction Pattern Showing Amorphous Condition of 450 Angstrom i-BN Film	4-12
4-12	TEM Image of 12,000 angstroms i-BN Film Showing Cubic BN Crystallites. SAD pattern (inset)	4-13
4-13	Various Literature IR Spectra for Boron Nitride	4-14
4-14	IR Spectra of Selected IBED i-BN Thin Films	4-16
4-15a	Raman Spectrum of Hexagonal BN Standard	4-17
4-15b	Raman Spectrum of Cubic BN Standard	4-17
4-16	Raman Spectrum of IBED i-BN	4-18
4-17	Representative Wear Track Profile and Associated Ball Wear (400X) for 440 C Stainless Steel Ball on i-BN System	4-20
4-18	Coefficient of Friction versus Sliding Distance (Si_3N_4)	4-20
4-19	Coefficient of Friction versus Sliding Distance (440 C)	4-21
4-20	SEM Micrograph Showing Adhesive Transfer to Coating #0317 Following Si_3N_4 Ball Test	4-22
4-21	SEM Micrograph of Wear Track for Sample #0626	4-22
5-1	Spectral Emittance of Boron Nitride on Etched Aluminum at 77 K and 200 K	5-2
5-2	Blow-off Scar of i-BN on Al Substrate Following Pulsed Electron Bombardment	5-3

LIST OF TABLES

Table		Page
3-1	Selected IBED i-BN Deposition	3-4
4-1	d-Spacing RATIOS* for the Boron Nitride System	4-13

SECTION 1

INTRODUCTION

The abrasive, adhesive and corrosive wear of conventional reciprocating and rotary engine components, such as face riding seals, has contributed to both a loss in efficiency and increased machinery downtime for periodic maintenance. This problem will only become more severe in the future with the development of advanced heat/adiabatic engines. The total economic impact of efficiency losses, downtime, and replacement parts is astounding. These conditions pose a serious and growing challenge to conventional lubrication technology to provide adequate lubrication at these higher temperatures. Thus there is an obvious and acute need to develop a materials system, surface treatment and solid coating which is self-lubricating and high temperature compatible.

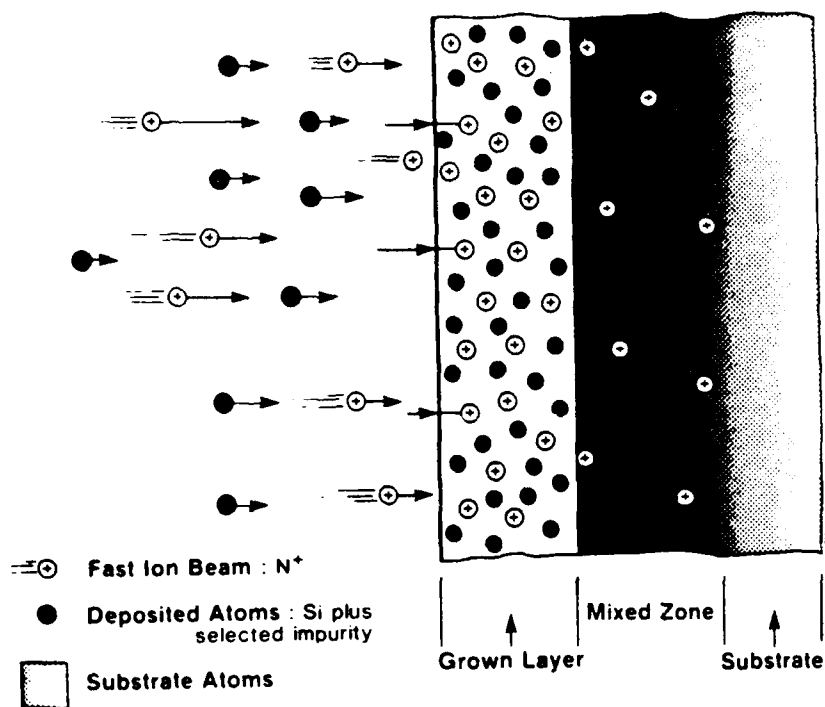
In applications where extreme high temperature operation (near 1000°C) is to be expected, such as adiabatic engines, all conventional lubricants either decompose, pyrolyze, or are simply inadequate. Conventional solid lubrications, such as molybdenum disulfide, suffer oxidative deterioration at temperatures over 250°C and even "diamond-like" carbon films begin to suffer oxidative deterioration as the temperature rises above 600°C. Many materials which are inherently self-lubricating are soft, lacking the strength necessary for structural members. Both carbon and BN have extremely hard cubic forms as well as lubricious forms, (graphite and hexagonal BN), which make them ideal wear-resistant, coatings for engine components. As applied by the novel technique of ion beam enhanced deposition (IBED), these coatings could possess a significant fraction of the cubic phase, which is extremely hard, wear-resistant, and has a low coefficient of friction. It is expected that under localized loading, microscopic thermal spikes would provide adequate energy to convert the metastable cubic form to the lubricious hexagonal form, thus generating a few atomic layers of solid lubricant at precisely the time and place required.

To produce a diamond-like coating of boron nitride which is both ultra-hard and adherent requires rather innovative technology. Cubic boron nitride is commercially produced in bulk form by the use of extremely high temperature and pressure which makes

these processes unsuitable for use with common engine materials. Furthermore, the process is completely unacceptable in applications where thin coatings are required. Through Spire's experience in materials research and high energy ion beam processing, the innovative method of IBED has been used to deposit coatings containing cubic boron nitride. The IBED process (shown in Figure 1-1) involves the use of an energetic ion beam of nitrogen impinging upon a substrate which is simultaneously being coated with evaporated boron. The effect is that the ion beam "mixes" the boron with the substrate material while at the same time forming boron nitride and providing energy for the growing layer in the form of thermal spikes. On a microscopic level these thermal spikes create the localized high temperature and pressure necessary for the formation of the cubic form of BN. Thus in the IBED process, as the individual ions strike the surface, the conditions used for the synthesis of macroscopic CBN structures are simulated. It is important to point out that on a macroscopic level the temperature of the substrate remains quite low and thus would not affect the tempering of various steels or alloys. The effect of the ion beam "mixing" is to eliminate material interfaces and associated mismatches by creating a graded transition between the substrate and the coated film.

The process of IBED is anticipated to become the process of choice for the application of adherent and hard tribological coatings. The coatings processed by this method are known to be extremely dense and free of pinholes and should prove to be of tremendous value as a chemical/mechanical protective surface.

PROCESS



ADVANTAGES

- LOW TEMPERATURE PROCESS
- SUPERIOR ADHESION AT INTERFACE
- AVOID COLUMNAR GROWTH
- IMPARTS COMPRESSIVE STRESS
- INCREASES NUCLEATION SITES
- NO THICKNESS LIMIT
- CONTROL OF STOICHIOMETRY

FIGURE 1-1. SCHEMATIC DIAGRAM OF THE IBED PROCESS.

SECTION 2 BACKGROUND

2.1 ION BEAM ENHANCED DEPOSITION (IBED)

The international ion beam R&D community has, in the past few years, given increased interest to the use of simultaneous ion bombardment and physical vapor deposition. Ion-assisted deposition has been reviewed by Harper et al. of IBM⁽¹⁾ and has been studied in several other laboratories⁽²⁻¹²⁾ since the mid-1970's to study electronic materials, to understand the role of ions in plasma-assisted deposition processes, to prepare dense optical coatings as well as to prepare tribological coatings. It is to be noted that most work in this area has utilized much lower energy beams (100 eV-2000 eV) than used in ion implantation.

There are several aspects of film growth that are beneficially influenced by ion bombardment during thin film deposition including: (i) adhesion, (ii) nucleation and growth, (iii) control of internal stress, (iv) morphology, (v) density, (vi) composition, and (vii) possibility of low temperature deposition.

Obviously, this process allows thicker alloyed regions to be attained than by either direct ion implantation or ion beam mixing but still incorporates advantages attributed to ion beams, such as superior adhesion due to precleaning and ion mixing during the initial stages of deposition. As an example, the adhesion of IBED optical coatings onto substrates has been improved by over an order of magnitude compared to results for deposition performed without ion beam assistance. Several researchers have also observed a significant reduction in the stress and crystallite size for ion assisted films.

IBED processing can also change the structure of deposited coatings. Conventional low temperature deposition processes often result in porous, columnar microstructures. This is a concern for optical coatings, for example, whose transmission properties are sensitive to the presence of absorbed water. It is commonly found that their characteristics in air and vacuum are different and that the use of ion bombardment

during the deposition can produce fully dense non-absorbing coatings whose characteristics are stable upon atmospheric exposure. Its use in depositing optical coatings is thus far the most advanced application area.

A number of studies⁽¹³⁾ have demonstrated how the internal stress within deposited films can be changed by ion bombardment during deposition, being attributed to a number of factors including: (i) impurity incorporation, (ii) the preferential sputtering-out of impurities, and (iii) thermal spike events.

IBED processing also allows control over stoichiometry and structure. For example, Si_xN_y coatings prepared by the IBED technique using silicon evaporation and low energy nitrogen bombardment can be continually varied from pure Si to stoichiometric Si_3N_4 by varying the relative ion beam and evaporant flux ratios. It is this type of control which motivated us to explore its use in producing (ion-assisted) i-BN.

2.2 APPLICATION TO NITRIDE FILMS

Previous studies^(3,13) have shown the IBED process capable of producing stoichiometric nitride films at room temperature. Weissmantel demonstrated that $\text{-Si}_3\text{N}_4$ films formed when the nitrogen beam current passed a critical threshold with respect to the silicon evaporant. Cuomo et al.⁽¹³⁾ also showed that AlN formed when the nitrogen to Al flux was above a critical value. In both of these cases any excess nitrogen appeared to be rejected.

2.3 PREVIOUS i-BN STUDIES

Weissmantel et al.⁽³⁾ were some of the first to publish on the production of hard boron nitride films by ion beams (reactive ion plating). They found a quasiamorphous structure via TEM with IR spectra confirming B-N bonding states and X-ray data consistent with crystallites of cubic boron nitride. They postulated that in the wake of the violent collision cascade of the stopping ions local high-temperature, high-pressure areas could be produced as shown schematically in Figures 2-1 and 2-2.⁽¹⁴⁾

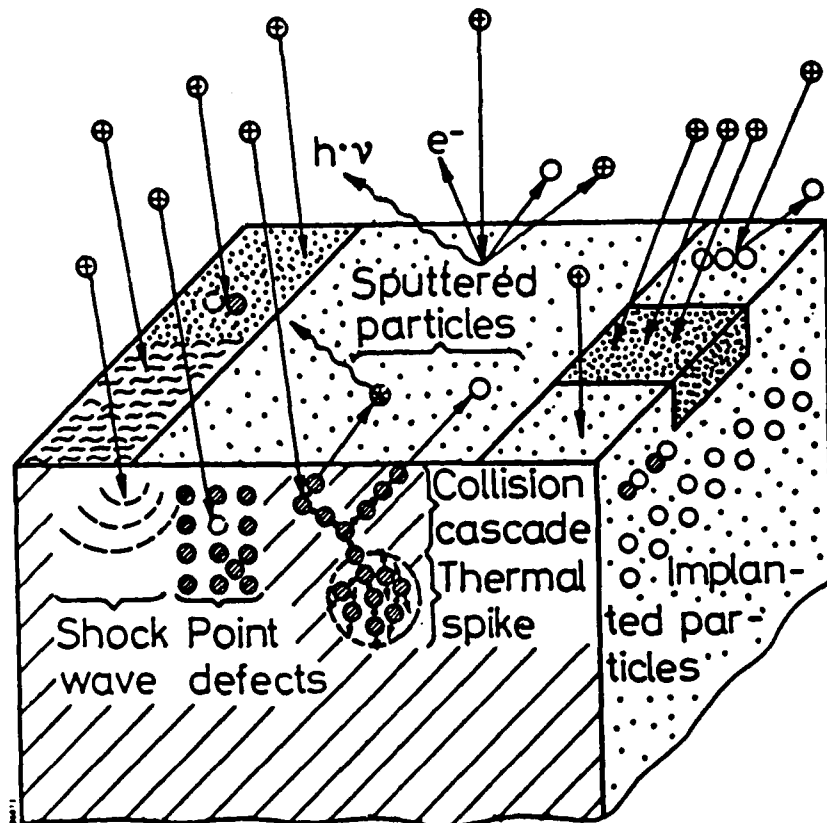


FIGURE 2-1. DEPICTION OF EVENTS INCLUDING DISPLACEMENT SPIKES OCCURRING DURING ION BOMBARDMENT OF A SURFACE. (C. Weissmantel)

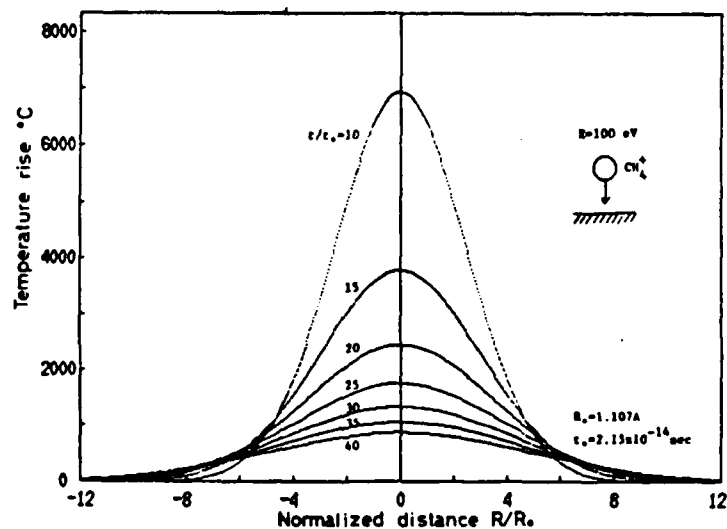


FIGURE 2-2. CALCULATED THERMAL SPIKE TEMPERATURE FOLLOWING ION BOMBARDMENT. (From Namba and Mori, Ref. 14)

Shortly thereafter Satou and Fujimoto published a short note⁽¹⁵⁾ claiming the formation of cubic boron nitride crystallites in an amorphous/hexagonal matrix. Their characterization consisted of electron micrography and electron diffraction. They evaporated boron and used a mass analyzed 40 keV N_2^+ beam (i.e., 20 keV N^+ ions). This work was continued,⁽⁷⁾ using additional analysis of IR absorption, X-ray diffraction and electron microscopy. They give evidence that films having a B/N ratio larger than 0.9 have a cubic boron nitride structure along with the hexagonal phase.

Recently Sainty et al.⁽¹⁶⁾ have published a comprehensive study using low energy (100 to 1500 eV) analyzed nitrogen beams on evaporated boron to produce boron nitride. Their films were characterized by EELS (electron energy loss spectroscopy), TEM, ellipsometry, and microhardness. They found no evidence of the cubic phase, but only the hexagonal phase present, in an extremely fine tangled network of ribbons of random orientation.

SECTION 3

PHASE II EXPERIMENTAL PROGRAM

Figure 3-1 shows a schematic of Spire's Ion Beam Enhanced (or Assisted) Deposition (IBED) system combining electron beam evaporation with simultaneous (nitrogen) ion bombardment. A Kaufman type ion source was used and operates from 200 eV to 1000 eV providing ion current densities up to 1000 microamps/cm².

In order to produce compounds combining evaporated material (B) with elements in the form of an energetic ion beam (i.e., nitrogen ions) one has to provide enough ions to ensure stoichiometry. Another consideration is that the non-mass-analyzed beam consists of a diatomic (N_2^+) component (approximately 90 percent abundant) as well as a monatomic (N^+) component (approximately 10 percent abundant). The diatomic component dissociates immediately upon striking the substrate with each nitrogen atom carrying away one-half of the initial beam energy. Both components will tend to sputter away surface atoms in competition with build-up from deposition. The ion-assisted deposition process is thus very complicated and models for predicting compound formation are only recently emerging.^(17,18)

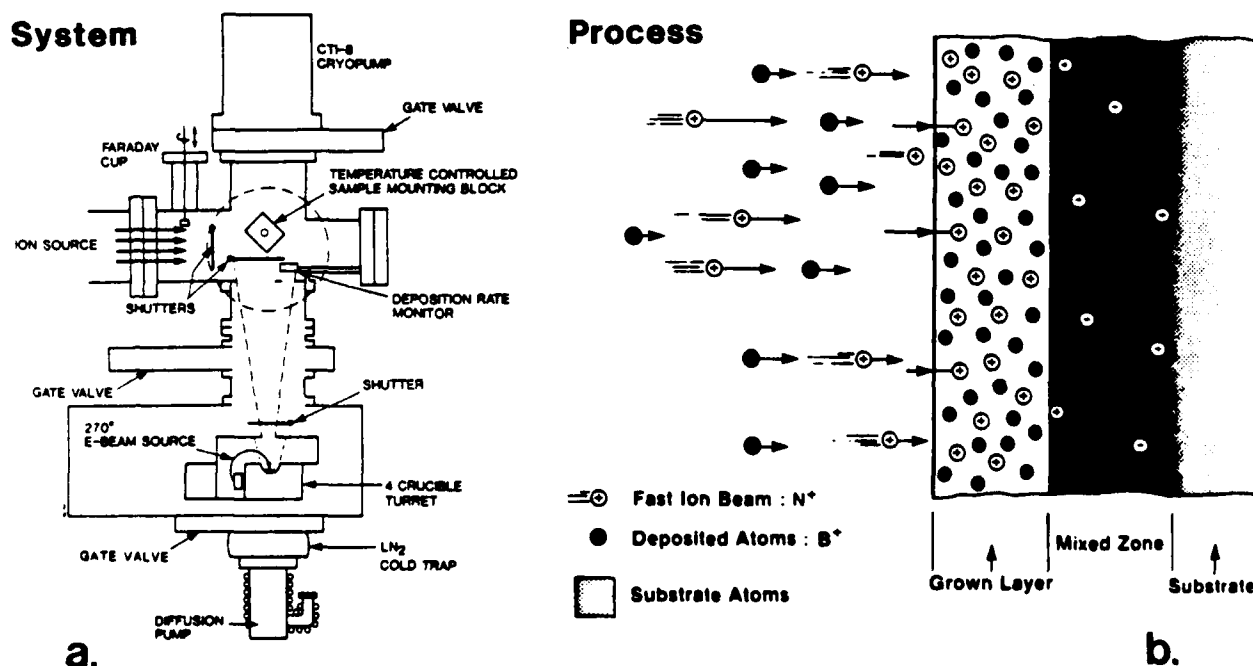


FIGURE 3-1. SCHEMATIC OF SPIRE'S ION BEAM ENHANCED (OR ASSISTED) DEPOSITION (IBED) SYSTEM (a) AND DEPICTION OF PROCESS (b) COMBINING ELECTRON BEAM EVAPORATION (BORON) WITH SIMULTANEOUS ION (NITROGEN) BOMBARDMENT.

The main experimental parameters include: (i) ion and evaporant species, (ii) the relative fluxes of the deposited material (e.g., B) and the ion species (e.g., N_2^+ plus N^+), and (iii) the substrate temperature. We have also found that other conditions such as background pressure and its makeup are also important affecting both the microstructure and properties of the resultant coating.

Spire's study of ion beam enhanced deposition of boron nitride (i-BN) systematically examined several properties of i-BN prepared over a range of boron to nitrogen arrival ratios (defined as R ratio) and for both low temperature and elevated substrate temperatures.

In the production of i-BN thin films by the IBED technique, the process parameters which are most relevant are the temperature of the substrate, the evaporation rate of the boron and the current density of the nitrogen ion beam at the substrate. Heating of the substrate due to the incidence of the ion beam alone typically results in a process temperature of 180° to 230°C for thin films (less than 1 micron) on non heat-sunk substrates. With the aid of a target stage heater, temperatures in excess of 400°C can be attained in the experimental chamber previously described. Evaporation rates for the boron are routinely in the range of 2 to 5 angstroms/sec for the films in this study and rate uniformity is generally kept within ± 0.3 angstroms/sec of the desired programmed rate by the crystal monitor.

Changes in the nitrogen ion arrival rate are possible by varying the current density of the ion beam as measured by a probe near the substrate surface. The present measurement system does not allow for a mass analysis of the beam (i.e., N_2^+ to N^+ ratio) nor does it take into account the effect on the current reading by secondary electrons emitted from the probe surface under ion bombardment. Further difficulty in identifying the "true" nitrogen arrival rate is due to the unknown neutral flux produced by charge exchange neutralization.

Recently, attempts have been made to quantify some of these factors^(18,19) using a Kaufman ion source of the type used in this study. A $N_2^+ : N^+$ ratio of 89 percent N_2^+ to 11 percent N^+ has been determined as average for a beam energy of 500 to 1000 eV; with the

neutralized fraction being 34 percent for beams of 500 eV in a working pressure of 2×10^{-4} torr. If a Faraday cup system equipped with a suppression bias is used to effectively eliminate the need to correct for a "secondary current," then a measured current density of 145 microamperes/cm² with a boron evaporation rate of 2 angstroms/sec reduces to a B/N arrival rate of 1:1 for this experimental geometry.

3.1 SPIRE'S i-BN STUDY

Table 3-1 is a listing of selected i-BN depositions done for this study. In total, the Phase I and Phase II efforts generated over 40 i-BN depositions over a large matrix of experimental parameters. In-house testing of Knoop microhardness as a function of load (grams) as well as ellipsometric determination of refractive index are routinely performed and are also listed here. Figure 3-2 illustrates a typical variation of microhardness with load as well as with incorporated B/N ratio of IBED i-BN thin films. Determination of the B/N ratio is done via nuclear reaction analysis using selected resonance reactions for boron and nitrogen and will be discussed in more detail later (see Section 4.1). Other in-house analyses include friction and wear behavior (see Section 4.5) and a more qualitative Moh's scratch hardness test (see Figure 3-3). It should be noted that this figure shows the general characteristics of the i-BN films; specifically, their ductile behavior (smooth, plastically deformed scratch edges) and their excellent adhesion to the substrate (no spalling or cracking along the scratch).

As evidenced by the data thus far presented, IBED i-BN thin films generally exhibit a high microhardness (KHN = 2000-3000, i.e. 20-30 GPa) and good adhesion to the substrate. Also notable are the thermal and chemical stability of these films.

3.1.1 Thermal Stability

The thermal stability of BN films has been studied by high temperature annealing. Figure 3-4 shows RBS spectra for a BN film on a Si substrate after (i) room temperature aging (2 months) and (ii) after a subsequent high temperature (750°C, 2 hours) annealing treatment.

TABLE 3-1. SELECTED IBED i-BN DEPOSITIONS.

Substrate	I (A/cm ²)	E (eV)	Rate (A/sec)	t (A)	Microhardness KHN @ (Load)	Refractive Index (n)
Si (100)	155- 160	600	2.0	3500	1980 (5g)	-
Si (100) and 304 stainless steel	430	700	1.5-2.0	8786	2200 (5g)	2.49-2.7
Si (100)	300	1000	2.0	6000	2400 (5g)	2.1
Si(100) @ 400°C	450	550	1.5	2500	3600 (5g)	2.08
Si (100) @ 400°C	425	500	1.5-2.0	2500	1900 (5g)	1.96-2.05
Si (100) @ 400°C	1000	1000	2.0-2.5	6000	2000 (5g)	2.15-2.46
Si (100) @ 400°C	1000	500	2.0-2.5	12000	2500 (25g)	2.13-2.7
Si (100)	200	600	2.0	12000	1650 (5g)	2.65
304 stainless steel	300	600	3.0	11000	1740 (5g)	-

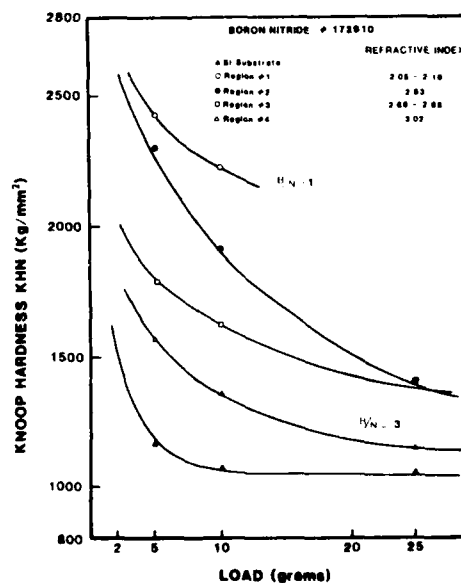


FIGURE 3-2. MICROHARDNESS VARIATION WITH B/N.



FIGURE 3-3. MOH'S #9 (Al_2O_3) SCRATCH ADHESION TEST ACROSS SILICON (left)/BN (right) BOUNDARY (10 g load).

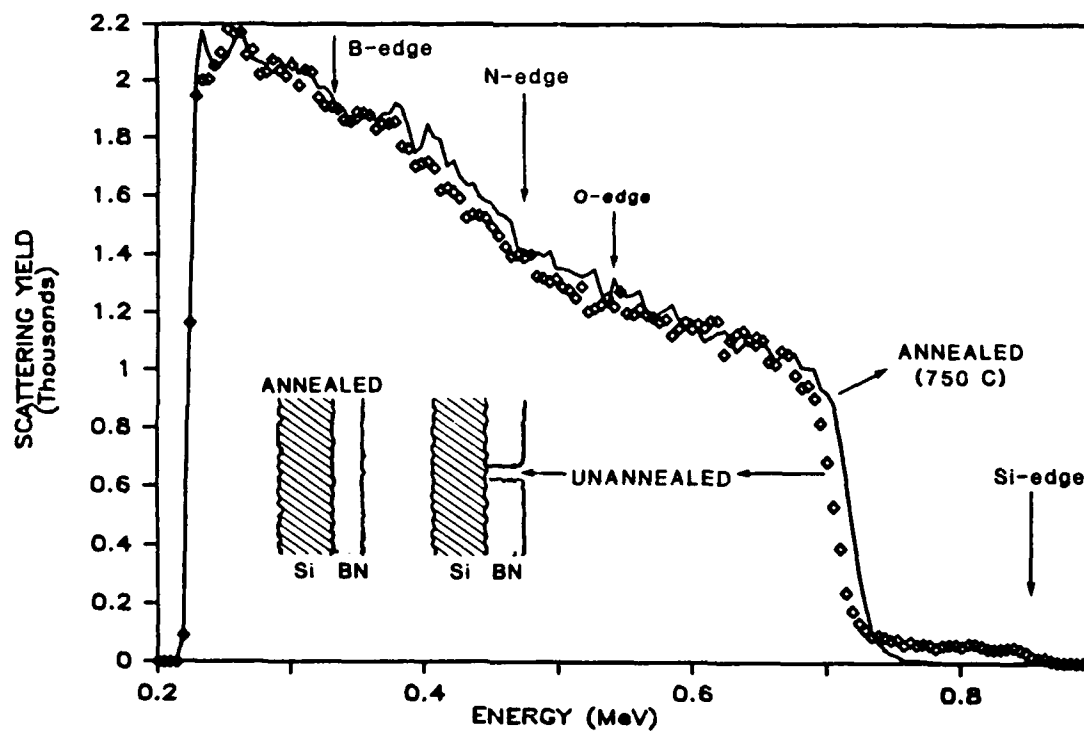


FIGURE 3-4. RBS SPECTRA OF UNANNEALED AND ANNEALED BN THIN FILMS (approximately 2000 angstroms) ON SILICON SUBSTRATE.

Although most of our IBED samples are free from any pinholes, in this particular sample (with a thickness of less than 2000 angstrom) RBS indicates the presence of pinholes in the unannealed condition. Upon annealing for 2 hours at 750°C in a nitrogen ambient, all of the pinholes filled up. On the other hand, RBS explicitly indicates that thin films become thinner as a result of annealing, indicating that during annealing some lateral diffusion occurs. However, no mechanical degradation has been observed for temperatures up to 900°C. RBS also shows little or no oxygen incorporation in this film either before or after the anneal, indicating the excellent resistance to oxidation which is characteristic of these i-BN films.

3.1.2 Chemical Stability

The best BN coatings were exposed to concentrated nitric acid for periods of several hours to days. Although the substrate material was clearly attacked by the acid, there were no visible changes in the appearance of the films, and no changes of the mechanical properties could be discerned in hardness measurements. BN coatings that had oxygen contamination, on the other hand, degraded quickly in appearance and hardness after a few days' exposure to atmospheric humidity and were quickly destroyed by exposure to acid. These results indicate the necessity of a clean vacuum environment to ensure film stability.

SECTION 4

EXPANDED ANALYSIS OF i-BN COATINGS

Since one of the key objectives of this program was the identification and optimization of the process parameters most relevant to the formation of cubic boron nitride, it was determined early in the program that a wider variety of analytical testing procedures would be needed to properly characterize these coatings. These "newer" techniques would be used in conjunction with the RBS and IR studies of the Phase I effort.

Strong activation involved in many ion beam assisted deposition processes does not only improve the quality and performance of stable compound films, e.g. titanium nitride, but also allows the formation of metastable structures with novel properties. Among these, diamond and diamond-like, as well as hard boron nitride films, are of special interest due to their many superior characteristics.

Deposition of compound films is generally complicated by the need to accurately control the composition. Ion beam processes, being normally far from the equilibrium conditions, require special attention in this respect. The increased chemical activity of ionized species also attracts many impurities, and contamination with carbon, oxygen, and hydrogen are common in many practical coatings.

In this study we have analyzed the boron and nitrogen concentrations in BN films produced by ion beam assisted deposition (i.e. i-BN films). It is assumed that the main properties of the films are determined by the boron to nitrogen ratio. That is why it is essential to know the effect of the process parameters on this ratio. In addition, impurities, especially hydrogen contamination, were examined. Hydrogen is known to possess the active role in hydrogenated i-C films occupying unfilled tetrahedral bondings.⁽²⁰⁾ In ion-plated hard BN films deposited using NH_3 gas, high concentrations of hydrogen have been observed.⁽²¹⁾ Moreover, IR spectroscopy has revealed H-B bonding in these films. For this reason, the incorporation of hydrogen could be expected also in the case where hydrogen is available only as a contaminant in the process.

4.1 NUCLEAR REACTION ANALYSIS (NRA)

The concentrations of boron and nitrogen were measured⁽²²⁾ using the nuclear resonance reactions $^{11}\text{B}(p,\gamma)^{12}\text{C}$ at $E_p = 163$ keV, and $^{15}\text{N}(p,\alpha,\gamma)^{12}\text{C}$ at $E_p = 429$ keV, respectively. The width of the $^{15}\text{N}(p,\alpha,\gamma)^{12}\text{C}$ resonance at $E_p = 429$ keV is extremely narrow, $\Gamma = 120$ eV, allowing precise depth profiling. In this case the depth resolution was determined by the energy resolution of the accelerator used, 400 eV (FWHM) at the energy involved. This corresponds to a depth resolution of 5 nm at the surface of the BN sample. The width of the $^{11}\text{B}(p,\gamma)^{12}\text{C}$ resonance at $E_p = 163$ keV is, on the contrary, very broad, $\Gamma = 5.7$ keV. In this case the depth resolution was determined by the width of the resonance alone. Consequently, the depth resolution of the boron profiling is only 40 nm at the surface of the BN sample. Because of the low energy of the $^{11}\text{B}(p,\gamma)^{12}\text{C}$ resonance the molecular beam H_2^+ at the acceleration voltage ≥ 326 keV was used. Both in the nitrogen and boron case the gamma-rays were detected using a NaI (Tl) detector $12.7 \times 10.2 \text{ cm}^2$ in size. The measured gamma-ray yields were converted into the absolute concentrations with the help of TiN and TiB_2 calibration samples respectively.

Hydrogen analysis was performed with the forward recoil spectroscopy technique (FRES)⁽²³⁾ using the He^+ beam at an energy of 2 MeV. For the determination of the absolute hydrogen incorporation the FRES spectrum from Kapton[®] was used together with the aid of computer program RUMP.⁽²⁴⁾ Complementary analyses of oxygen and carbon were carried out utilizing the deuterium reactions $^{12}\text{C}(d,p)^{13}\text{C}$, $^{16}\text{O}(d,p)^{17}\text{O}$, and $^{16}\text{O}(d,\alpha)^{14}\text{N}$ (25,26) at the energy of $E_d = 925$ keV.

The nitrogen, boron, and hydrogen analyses were performed on all samples, whereas the carbon and oxygen analyses were carried out only on selected samples.

*Kapton is a registered trademark for a polyimide material manufactured by DuPont Electronics, Wilmington, DE.

4.1.1 Results and Discussions

Shown in Figures 4-1 and 4-2 are examples of nitrogen and boron distributions in two different i-BN films. The sample #1103 can be found to be formed mainly of the main constituents boron and nitrogen with the average ratio $[B]/[N] = 1.5$. In the case of the sample #0626 the nitrogen distribution is very inhomogeneous and the sum of the boron and nitrogen concentrations deviates remarkably from 100 percent. This indicates the presence of an extra constituent (i.e., carbon) which was verified later with deuterium measurements.

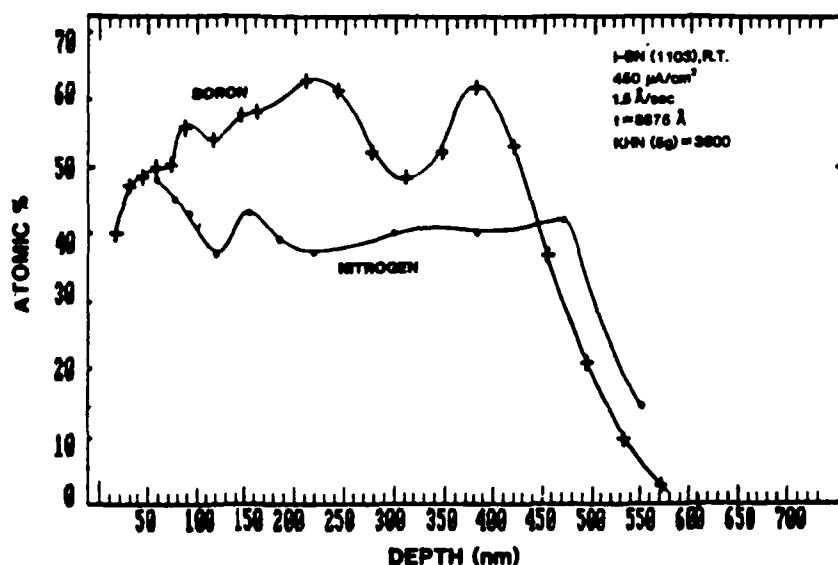


FIGURE 4-1. NITROGEN AND BORON DISTRIBUTIONS IN THE SAMPLE #1103.

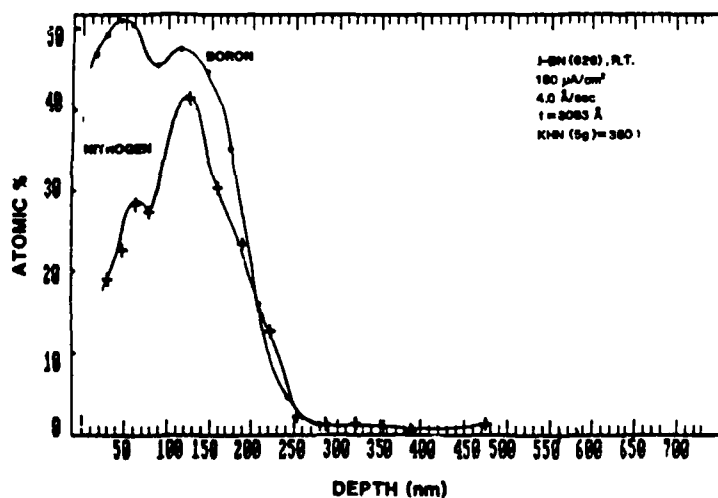


FIGURE 4-2. NITROGEN AND BORON DISTRIBUTIONS IN THE SAMPLE #0626.

The hydrogen contamination varied strongly. In most cases the contamination was small but detectable, e.g. 0.2 - 2.0 at. percent. The surface contamination, however, was always very pronounced. In Figure 4-3 can be seen the FRES spectra from the samples #0626 and #0121. The hydrogen contamination of the former sample was the smallest of the samples examined. The incorporation of hydrogen in the sample #0121 was the highest observed, and the average concentration corresponds to 12 at. percent. The high hydrogen concentrations ([H] 3.0 at. percent) were measured in three samples, two of which were deposited at the elevated temperature (400°C).

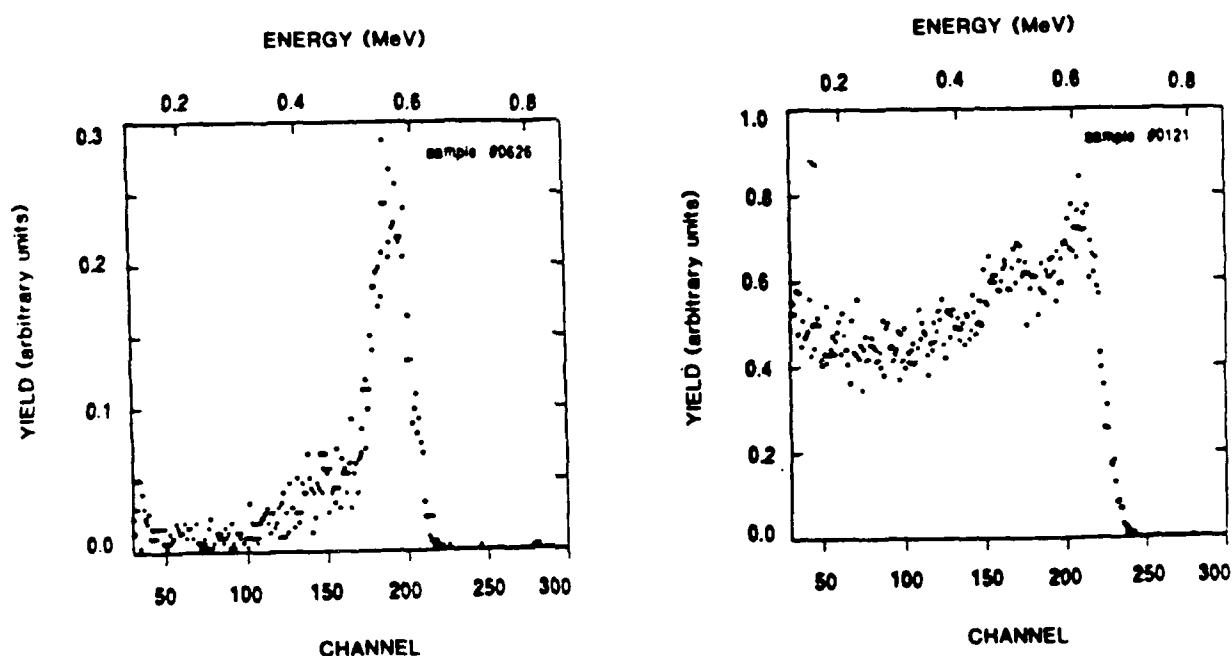


FIGURE 4-3. FRES SPECTRA OF THE SAMPLES #0626 and #0121.

Deuterium induced particle spectra were also taken from some selected samples. Shown in Figure 4-4 are the spectra from the samples #0626 and #0121. The signals from different elements are indicated in the figure. The most striking feature in the case of the sample #0626 is the strong signal from the $^{12}\text{C}(\text{d,p})^{13}\text{C}$ reaction. Because the sum of boron and nitrogen in this sample was much less than 100 percent (Figure 4-2), it can be concluded on the basis of Figure 4-4 that carbon is the third main constituent of this film. This carbon contamination has been subsequently traced back to originating from the electron beam inadvertently striking the graphite crucible containing the boron evaporation charge.

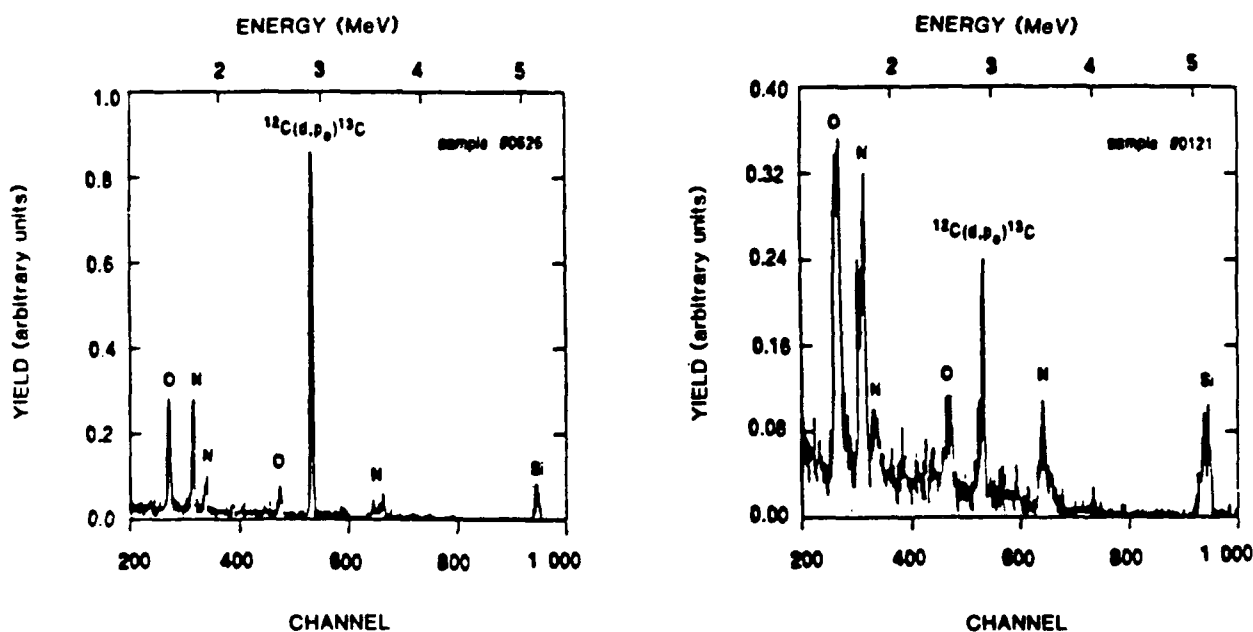


FIGURE 4-4. DEUTERIUM INDUCED PARTICLE SPECTRA OF THE SAMPLES #0626 AND #0121.

The highest level of hydrogen contamination (i.e. 12 at. percent) was seen in sample #0121 and is attributed to contamination from residual water vapor and hydrocarbons in the vacuum.

In both samples of Figure 4-4, detectable amounts of oxygen are visible. The oxygen signal was very small in all samples corresponding to only a few percent. However, in the case of the sample #0121 with the high hydrogen contamination the oxygen signal is slightly stronger indicating that at least part of the hydrogen originates in water vapor and that some water is incorporated in the film.

To relate the composition of the samples to the deposition conditions the $[B]/[N]$ ratio was plotted as a function of the quantity R defined as:

$$R = \frac{\text{ion beam current density } (\mu\text{A}/\text{cm}^2)}{\text{arrival rate of evaporant } (\text{\AA}/\text{s})}$$

In Figure 4-5 the data for the depositions at low temperature as well as elevated temperatures are shown. In the low temperature case, only the samples with the low contamination level and reliable analysis were involved, whereas in the case of the elevated temperature, all three samples have been taken into account. The general tendency, as can also be expected, in both cases is the increasing $[B]/[N]$ ratio with the decreasing R . In almost all cases the hyperstoichiometric boron concentration was observed. This is consistent with the observation of Weissmantel et al., who reported the boron concentrations from almost 100 percent to 50 percent in their i-BN films fabricated with the ion-plating technique.⁽³⁾ Moreover, as can be seen in Figure 4-5 a higher temperature seems to favor the hyperstoichiometric boron concentrations.

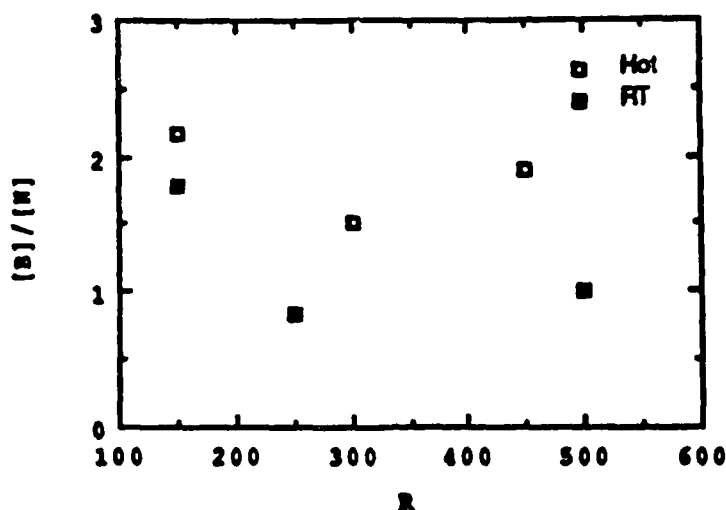


FIGURE 4-5. THE DEPENDENCE OF THE $[B]/[N]$ RATIO ON THE DEPOSITION PARAMETERS.

The chemical composition of the i-BN films seems to have good correlation with the mechanical properties and this is discussed in Section 4.5. It is interesting to note that the sample with the highest carbon contamination possesses the best tribological properties. This was thought to be due to the formation of boron carbide; however, ESCA analysis does not indicate B-C bonding in the form of B_4C .

4.1.2 Conclusions

A comprehensive chemical analysis based on the ion beam methods has been performed on several i-BN films. All films (except one) had the hyperstoichiometric boron concentration. The ratio $[B]/[N]$ approached the theoretical value at the highest current densities of the nitrogen beam.

In three samples high hydrogen contamination was found although pure nitrogen was used in the ion source. This impurity level is related to the mechanical behavior of the films. In one case, high carbon contamination was observed and correlates with improved mechanical properties.

4.2 AUGER AND XPS ANALYSIS

Results from NRA of IBED i-BN films (Section 4.1) indicate that many films are hyperstoichiometric (boron rich) as confirmed by Auger spectroscopy and XPS (ESCA) analysis.

An Auger spectrum of a cubic boron nitride reference sample (General Electric "BORAZON") appears in Figure 4-6(a). Figures 4-6(b) and 4-6(c) are spectra from an IBED i-BN film and show an apparent increase in boron enrichment with depth. An XPS depth profile of a similarly prepared BN film (Figure 4-7) also illustrates the hyperstoichiometric condition (B/N ratio) varying in the range of 2 to 3.

Included with the XPS survey is an interesting analysis which indicates that the relative amounts of boron nitride and elemental boron change several times throughout the depth profile. Figure 4-8 shows a three-dimensional montage of the boron (1s) binding energy peak as a function of depth in an IBED i-BN film. The high binding energy peak is due to boron in a B-N binding state, while the lower peak is attributable to elemental boron. The peak position varies depending upon the relative concentrations of BN and B

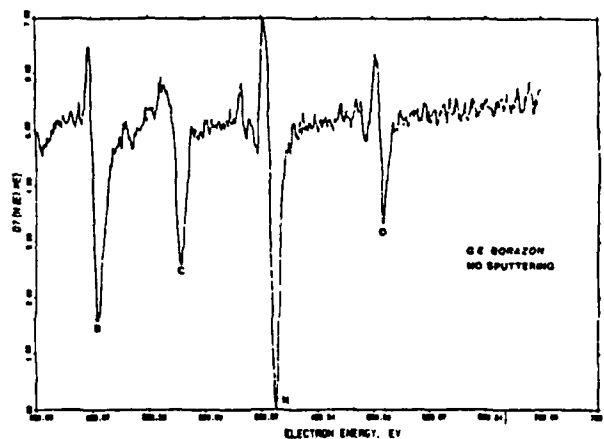


FIGURE 4-6(a). AES DATA FOR G.E. CBN REFERENCE SAMPLE.

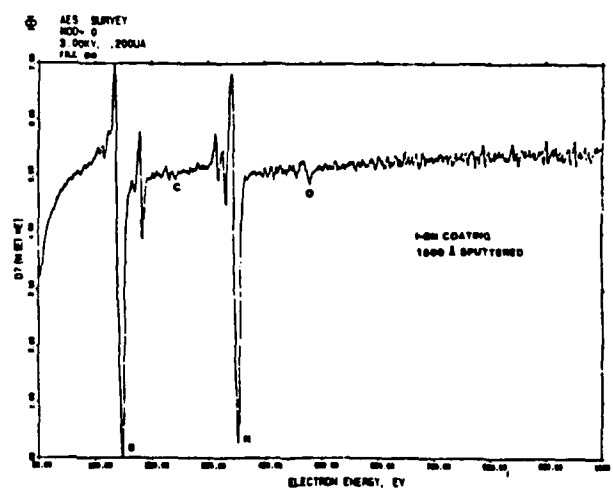


FIGURE 4-6(b). AES DATA FOR i-BN COATING (1500 angstroms sputtered).

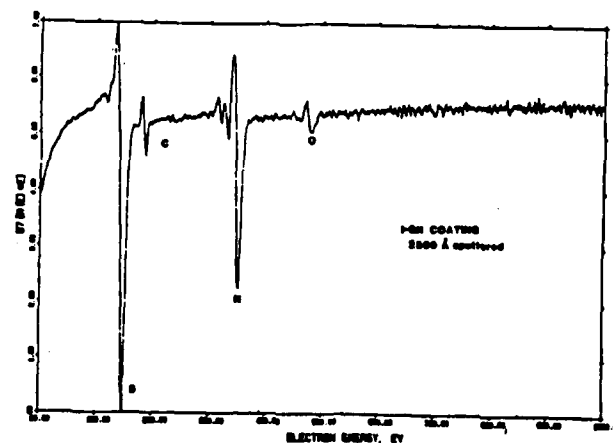


FIGURE 4-6(c). AES DATA FOR i-BN COATING (2500 angstroms sputtered).

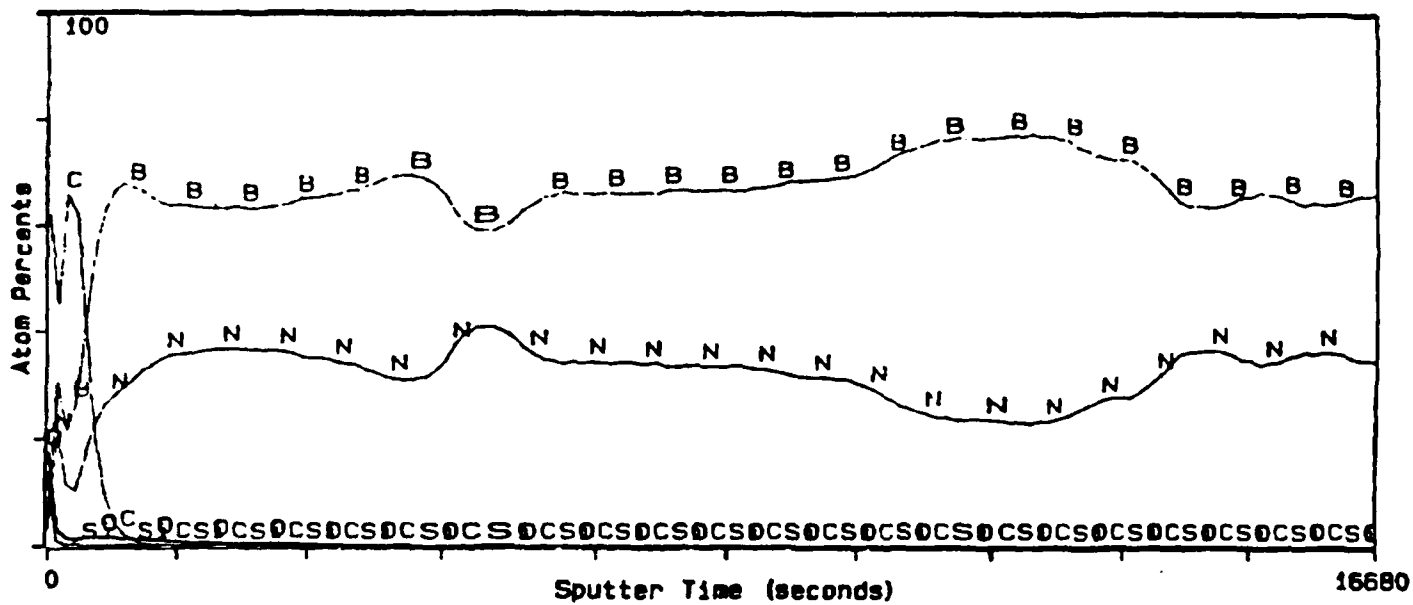


FIGURE 4-7. XPS DEPTH PROFILE OF IBED i-BN COATING.

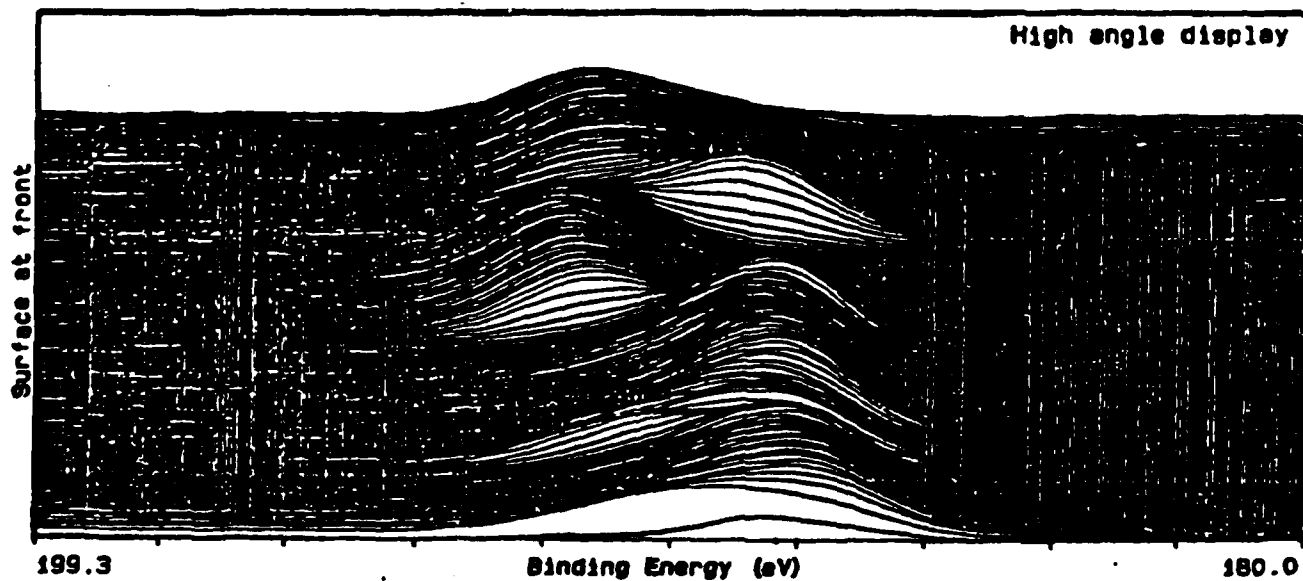


FIGURE 4-8. THREE-DIMENSIONAL MONTAGE OF BORON (1s) BINDING ENERGY PEAK AS A FUNCTION OF DEPTH IN IBED i-BN.

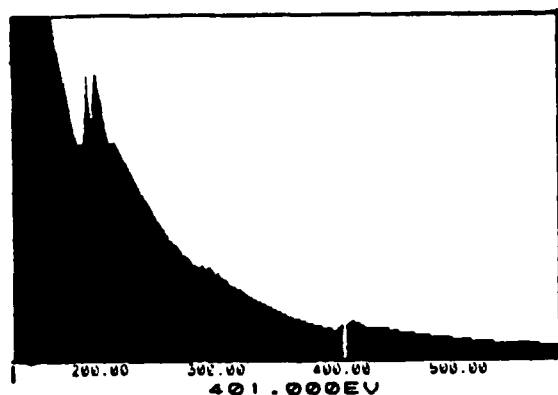
present at that depth. It is not known at this time whether these variations are due to subtle changes in the growth dynamics of the BN system or whether they are the result of non-uniformities in the atomic arrival rate ratios of the various reactive species involved (i.e., B, N_2^+ , N^+ , N_2^0).

4.3 STRUCTURE AND CRYSTALLINITY

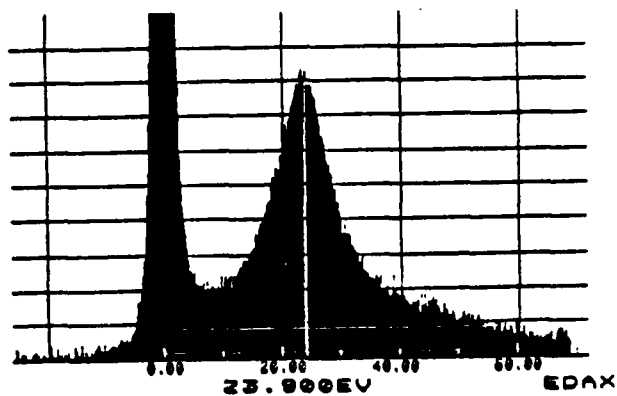
The boron nitride system has many similarities to the naturally occurring carbon system. Boron nitride exists in a soft, lubricious hexagonal phase (similar to graphite) as well as the super-hard cubic phase (similar to diamond). A weakly bonded, layered network of trigonally coordinated (sp^2) sites is found in the former while the latter consists of tetrahedrally coordinated (sp^3) sites which account for its many unique physical properties. Both systems can exist (less commonly) in a tetrahedrally coordinated, hexagonal close-packed structure known as wurtzite type.

Electron energy loss spectroscopy (EELS), and transmission electron microscopy (TEM) with selected area diffraction (SAD) analyses have been performed on selected i-BN samples in this study in an attempt to identify the crystalline nature of these films. There is some evidence to suggest that there may be differences in the nucleation process for crystallite growth between thin (approximately 450 angstrom) and thick (12,000 angstrom) films, since films of these thicknesses deposited under identical conditions are quite different in TEM. While a more detailed investigation into this hypothesis is being conducted, we present some preliminary results here.

A thin film of i-BN (450 angstroms) was examined by EELS and TEM/SAD. Both techniques confirmed a featureless, amorphous matrix of BN. The EELS measurements in the core electron excitation region and the plasmon-loss region shown in Figure 4-9 agree well with those of a BN (hexagonal) standard Figure 4-10. Location of the B-K edge and N-K edge and the position of the main plasmon peak at 23.9 eV are indicative of a loosely packed hexagonal BN structure. The diffraction pattern (Figure 4-11) for this thin film indicates an amorphous structure and the TEM image was featureless and showed no crystallites.

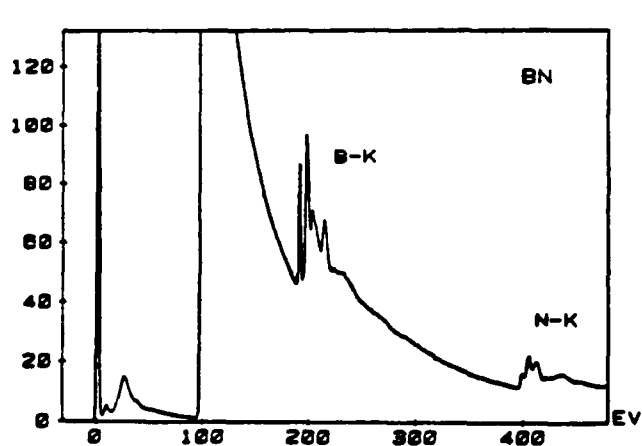


a

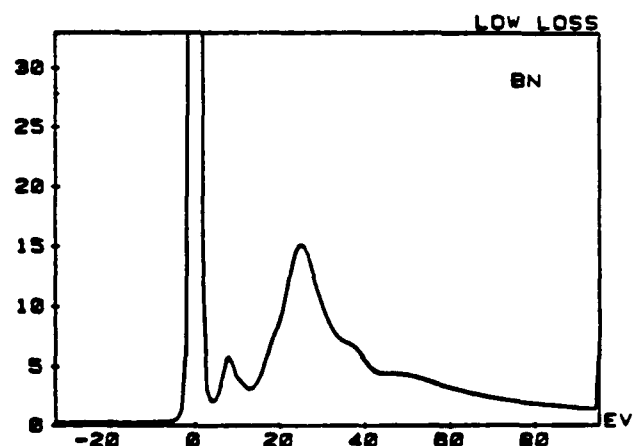


b

FIGURE 4-9. CORE ELECTRON EXCITATION REGION (a) AND PLASMON LOSS REGION (b) FOR IBED I-BN COATING.



a



b

FIGURE 4-10 CORE ELECTRON EXCITATION REGION (a) AND PLASMON LOSS REGION (b) FOR HEXAGONAL BN STANDARD.

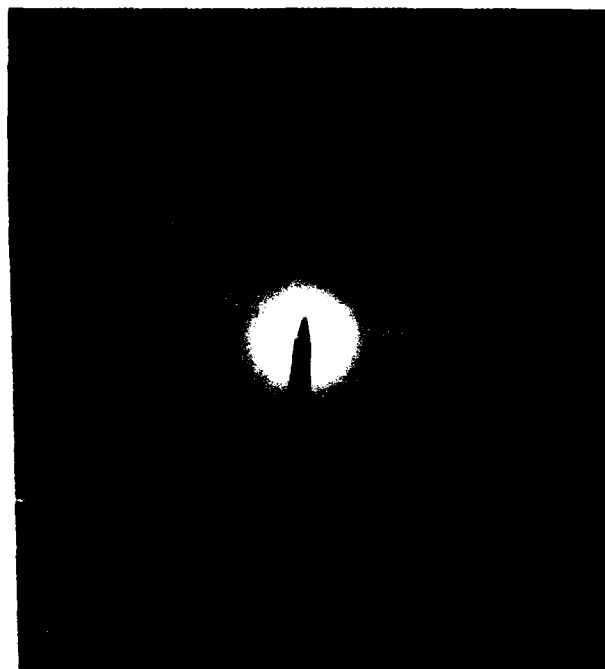


FIGURE 4-11. DIFFRACTION PATTERN SHOWING AMORPHOUS CONDITION OF 450 ANGSTROM i-BN FILM.

In contrast to the thin film characteristics, a thicker film (12,000 angstrom) was similarly analyzed by TEM/SAD and indicated a more structured system with crystallites of 200-500 angstrom cross section present. Figure 4-12 shows the TEM image and the associated SAD pattern. Analysis of the d-spacing ratios from this pattern is given in Table 4-1 and clearly indicates the crystallites to be cubic BN.

Further work needs to be done in the investigation of how process parameters affect the nucleation and growth of second phase crystallites. The observed lack of precipitates for thin films (450 angstroms) vs. the results shown in Figure 4-12 makes it tempting to attribute the nucleation to be thickness or stress dependent.

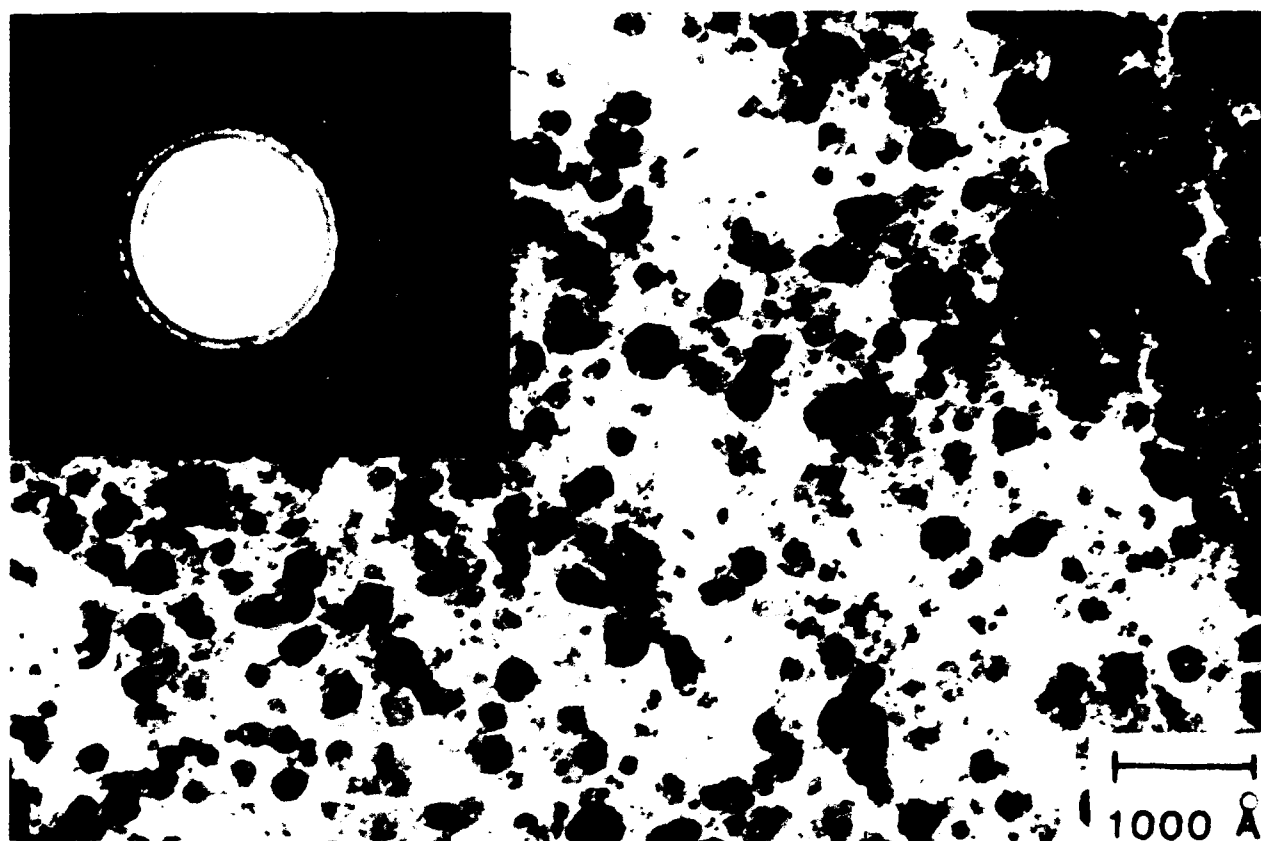


FIGURE 4-12. TEM IMAGE OF 12,000 Å i-BN FILM SHOWING CUBIC BN CRYSTALLITES. SAD pattern (inset).

TABLE 4-1. d-SPACING RATIOS* FOR THE BORON NITRIDE SYSTEM

IBED i-BN	Cubic BN	Hex. BN	Wurtzite BN
1.153	$\frac{(111)}{(200)}=1.154$	$\frac{(002)}{(100)}=1.534$	$\frac{(100)}{(002)}=1.046$
1.636	$\frac{(111)}{(220)}=1.632$	$\frac{(002)}{(101)}=1.614$	$\frac{(100)}{(101)}=1.129$
1.909	$\frac{(111)}{(311)}=1.915$	$\frac{(002)}{(102)}=1.831$	$\frac{(100)}{(102)}=1.447$

* Ratios for cubic BN derived from JCPDS card #35-1365. Ratios for hexagonal BN derived from JCPDS card #34-421. Ratios for wurtzite structure BN derived from JCPDS card #26-773.

4.4 INFRARED AND RAMAN SPECTRA ANALYSIS

IR transmission spectra for BN are prevalent in the literature (see Figure 4-13) for films which were deposited by a variety of methods. There is moderate agreement among investigators in the interpretation of these spectra with regard to the significance and location (wavenumber) of the major peaks, although the inconsistencies are enough to suggest that IR measurements alone are not sufficient to conclusively identify the crystal structure of a BN sample.

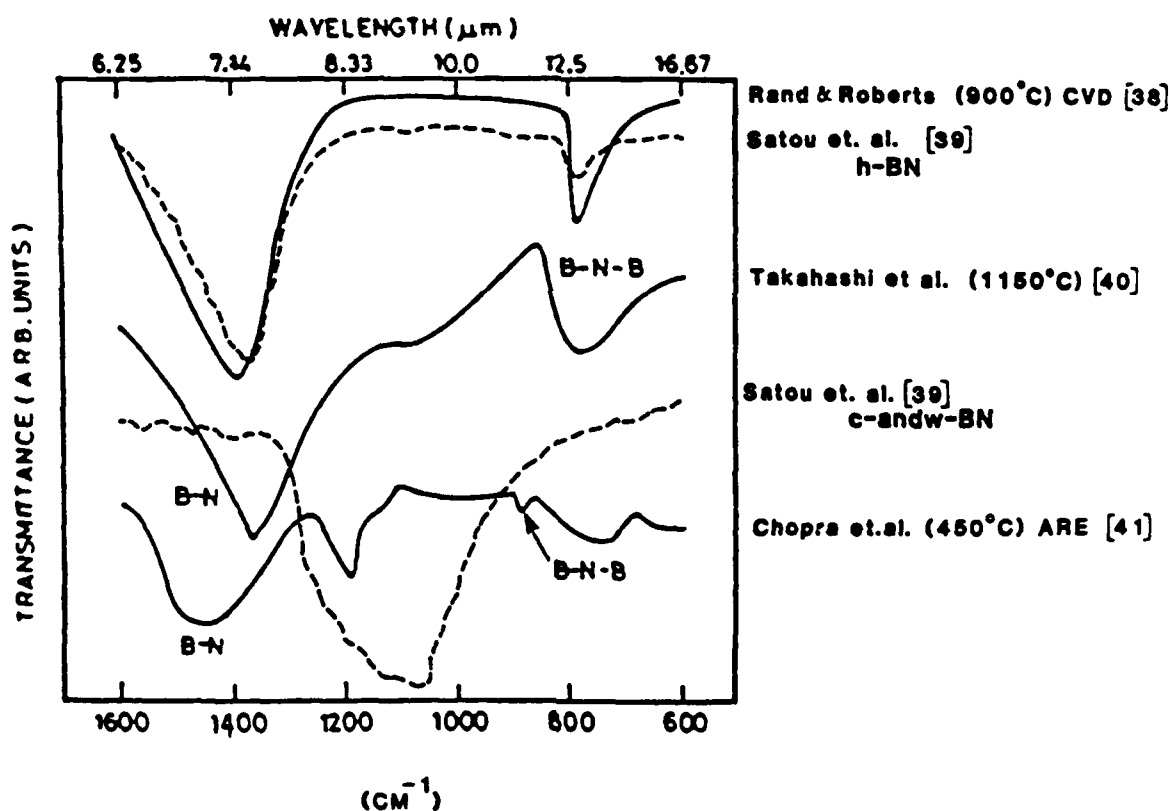


FIGURE 4-13. VARIOUS LITERATURE IR SPECTRA FOR BORON NITRIDE.

There are two peaks, however, which are generally attributed to be indicative of hexagonal phase BN. One rather broad peak is in the 1370 cm^{-1} to 1400 cm^{-1} range and is attributed to B-N bond stretching (in plane) while the other (usually smaller and somewhat more well defined) is located in the 750 cm^{-1} to 780 cm^{-1} range and is associated with B-N-B bending (out of plane). Occasionally seen are peaks at 2500 cm^{-1} (B-H bonds) and 3430 cm^{-1} (hydroxyl impurities or NH_2 groups) in films prepared by CVD type methods.

Among the smaller group of investigators who have claimed to identify cubic BN, there is more disagreement in the identification of peaks specific to the cubic phase. Some researchers^(31,32) attribute the peaks just mentioned (i.e., 1400 cm^{-1} and 800 cm^{-1}) to cubic phase, while others using reactive diode sputtering⁽³³⁾ attribute a peak that shifts from 810 cm^{-1} to 785 cm^{-1} with increasing bias to denote c-BN. Adding to the uncertainty are those findings^(34,35) that claim a peak at 1050 cm^{-1} to 1100 cm^{-1} is characteristic of cubic BN.

Results of a study by Spire on selected IBED i-BN thin films are shown in Figure 4-14 and suggest a cubic phase (crystallites) in a hexagonal matrix due to peaks at 1100 cm^{-1} and 1400 cm^{-1} , 750 cm^{-1} , respectively. As mentioned in Section 4.3, this has been confirmed by TEM/SAD analysis.

In contrast to the conflicting interpretations which abound in IR studies of boron nitride, Raman spectroscopy appears to afford a clearer distinction between the structural phases (cubic vs. hexagonal) of this system.

Although the presence of peaks and their positions in the IR and Raman spectra of a material are often similar, they need not be so and indeed a substance may be inactive in infra-red and active in Raman. This difference is due to the fact that IR spectra are more dependent on molecular vibrations involving a change in dipole moment of the molecule, whereas Raman spectra are sensitive to changes in the polarizability of a molecule. As an example consider Cl_2 , whose molecular vibrations, by symmetry, involve no net displacement of charge (dipole moment) and is therefore inactive in infra-red. However, the polarizability does change (with bond length) during vibration, and thus Cl_2 is active in Raman.

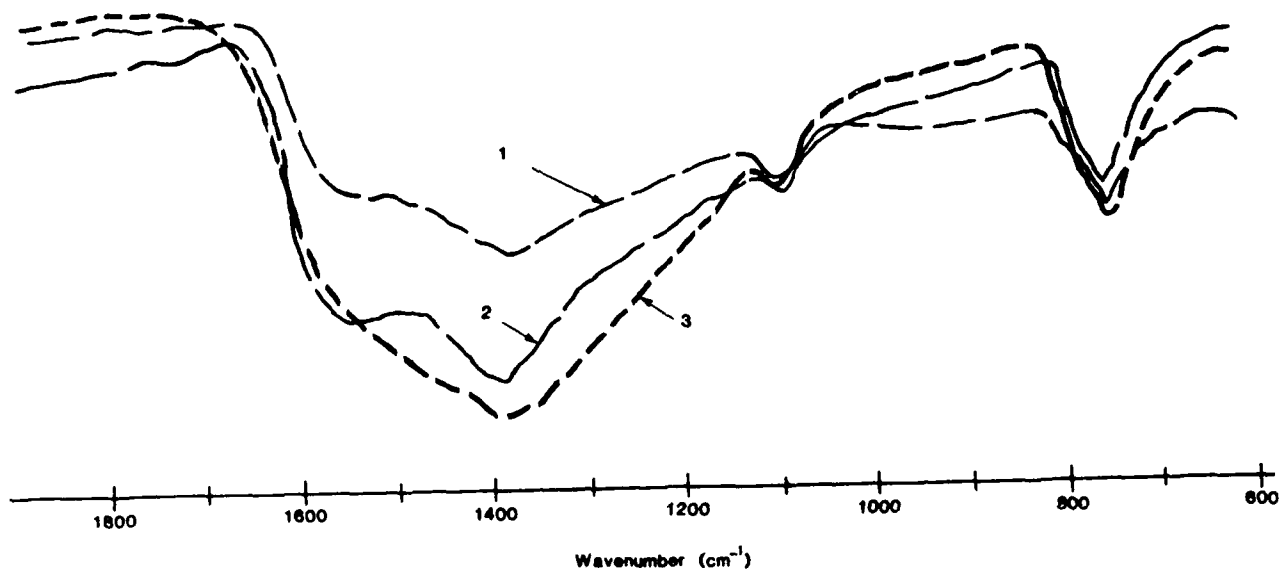


FIGURE 4-14. IR SPECTRA OF SELECTED IBED i-BN THIN FILMS.

Figure 4-15(a) shows a Raman spectrum of a hexagonal-BN standard with characteristic peak at 1366 cm^{-1} . Figure 4-15(b) is the Raman of a cubic-BN standard showing the two characteristic peaks at 1055 cm^{-1} and 1306 cm^{-1} . The two spectra are clearly different. Figure 4-16 shows the Raman of an IBED i-BN film. A small peak at 1300 cm^{-1} is present while no peak is visible at the h-BN position of 1366 cm^{-1} . The spectrum suggests a cubic phase BN. The absence of the other cubic peak may be due to the fact that ratios of intensities of the two peaks (LO to TO modes) have been found to be as great as 10 in zincblende type crystal structures,⁽³⁶⁾ and at the very least have been found to be dependent on many factors.⁽³⁷⁾

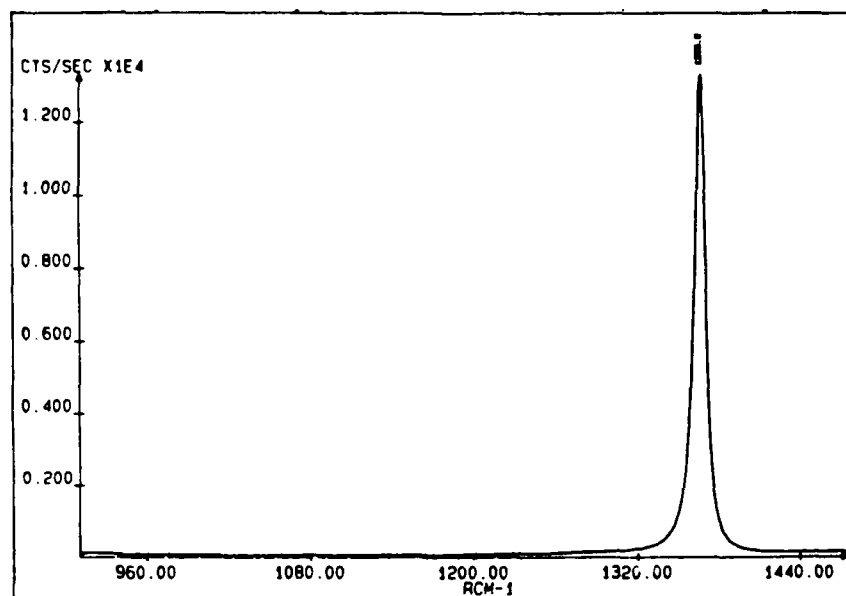


FIGURE 4-15(a). RAMAN SPECTRUM OF HEXAGONAL BN STANDARD.

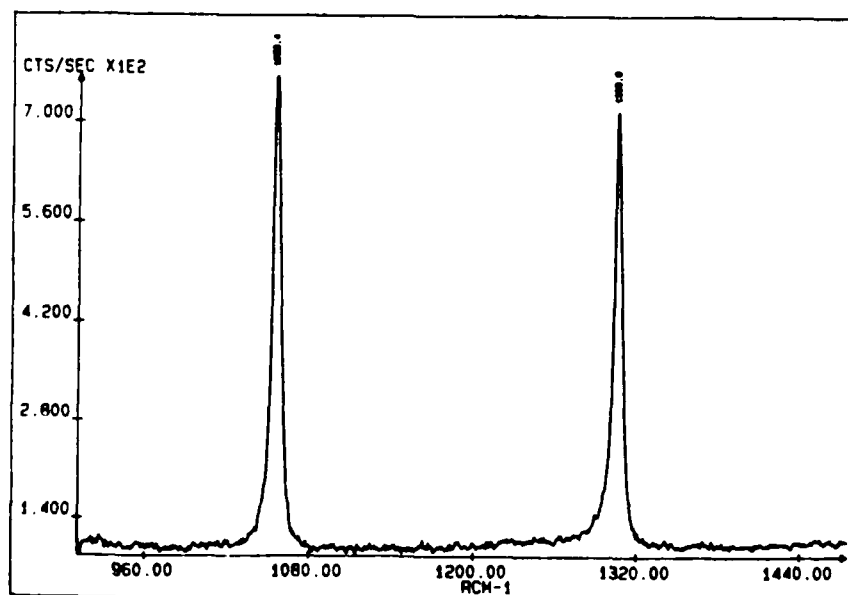


FIGURE 4-15(b). RAMAN SPECTRUM OF CUBIC BN STANDARD.

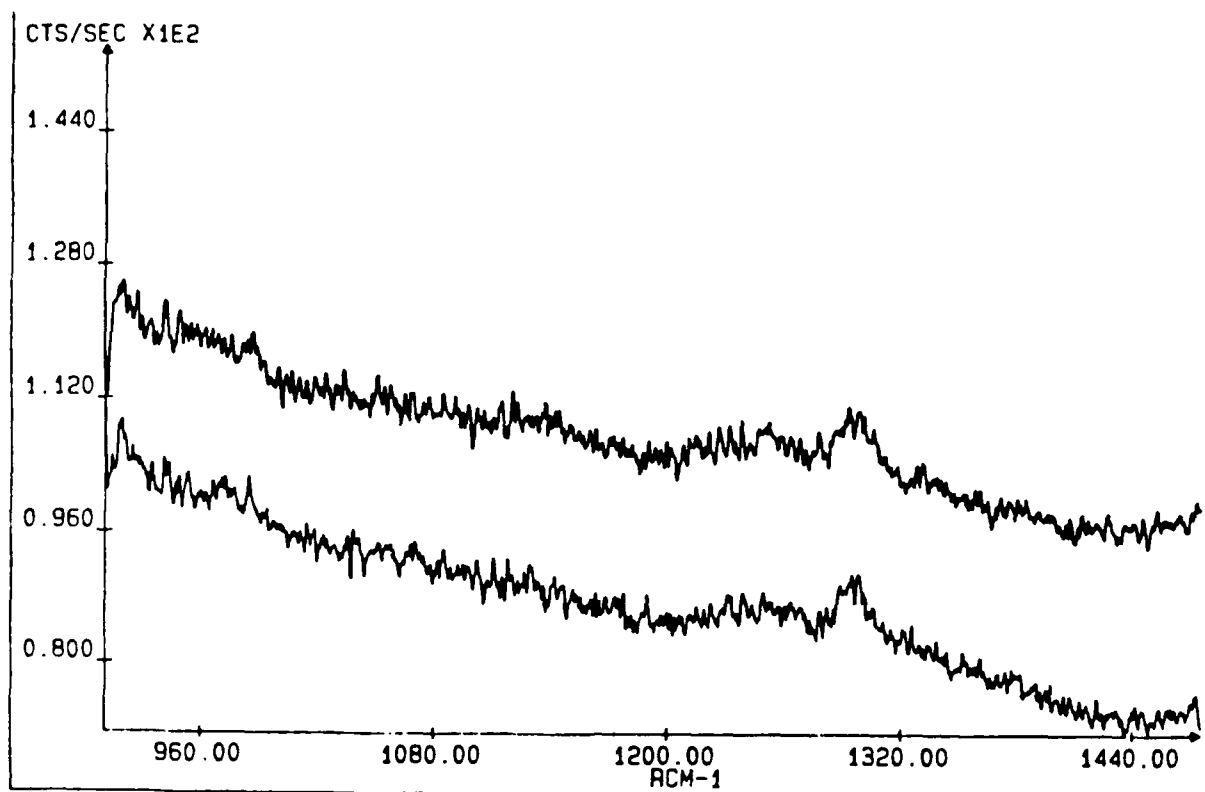


FIGURE 4 16. RAMAN SPECTRUM OF IBED i-BN.

4.5 FRICTION AND WEAR BEHAVIOR

Because of their high hardness and refractory nature, many nitride compounds are excellent candidates for coatings in a variety of high mechanical and/or thermal stress applications.⁽³⁸⁾ Other advantageous characteristics for a tribological coating would be excellent adhesion to its substrate as well as low friction and wear against a variety of counterface materials.

IBED i-BN films are being studied for their friction and wear behavior because the IBED process, as described earlier, characteristically produces highly adherent coatings and boron nitride as a material offers many unique properties especially in its cubic phase.

The friction and wear behavior of the coatings were investigated using an in-house built ball-on-disc apparatus. The test sequence involves a combination of adhesive and abrasive wear. Either continuous circular motion or reciprocating line motion of ball on coating is possible. Ball materials compared were silicon nitride and 440C stainless steel. All tests were run unlubricated in air, on coatings which were deposited on Si (100) wafers.

The load on the ball normal to the test sample can be varied by means of adding calibrated mass to the weight pan. During testing, the test stage is moved beneath the stationary loaded ball and the horizontal displacements of the ball/lever arm assembly are recorded on a strip chart recorder from the output of a load cell in the lever arm. Prior to the test, the recorder output is calibrated under a known load/displacement so that under the true test conditions the recorded signal yields the friction force of the ball/coating system. The coefficient of friction, μ , can now be calculated as the ratio of the normal force to the friction force.

The wear for the various systems was evaluated by measuring the depth profile of the wear scar seen on the coating using a Dektak profilometer and comparing it to the size of the wear flat on the ball surface under microscopic inspection. A new ball surface was used for each test. Estimates of coating volume loss were made from the wear scar profile and scar length (approximately 2 mm). By measuring the diameter of the contact area of the ball, the volume loss of the ball can be calculated in a manner similar to Hartley.⁽³⁹⁾ A dimensionless wear parameter, K, can be derived for the ball following Archard:⁽⁴⁰⁾

$$K = 3H(\Delta V)/Ns$$

where H, ΔV , N and s are respectively the hardness of the ball (KHN = 700), the volume loss of the ball, the load, and the sliding distance. Figure 4-17 shows a typical wear track profile and associated ball wear flat.

The variation in coefficient of friction with sliding distance is summarized in Figures 4-18 and 4-19 for the Si_3N_4 ball and the 440C ball respectively. Additionally Figure 4-18 includes the boron to nitrogen ratio of the i-BN films determined by nuclear reaction resonance analysis as well as a qualitative mention of hydrogen content, [H], from forward recoil spectrometry (Section 4.1). Figure 4-19 includes the wear parameter, K, for the 440C systems investigated, as well as estimates of coating volume loss.

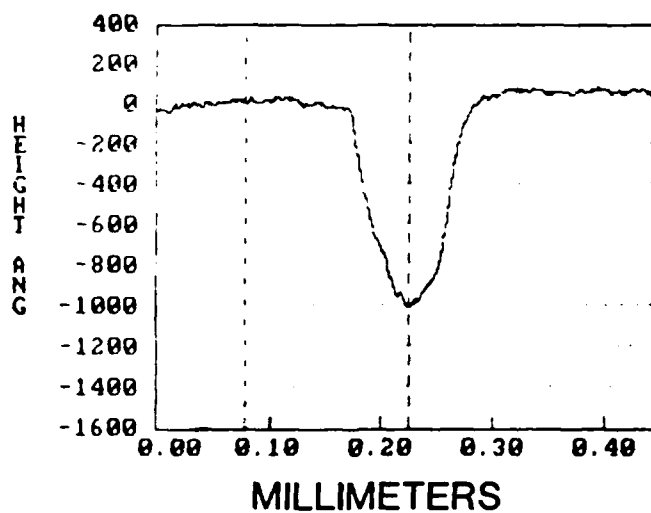


FIGURE 4-17. REPRESENTATIVE WEAR TRACK PROFILE AND ASSOCIATED BALL WEAR (400X) FOR 440 C STAINLESS STEEL BALL ON i-BN SYSTEM.

Si₃N₄ ball (dry)

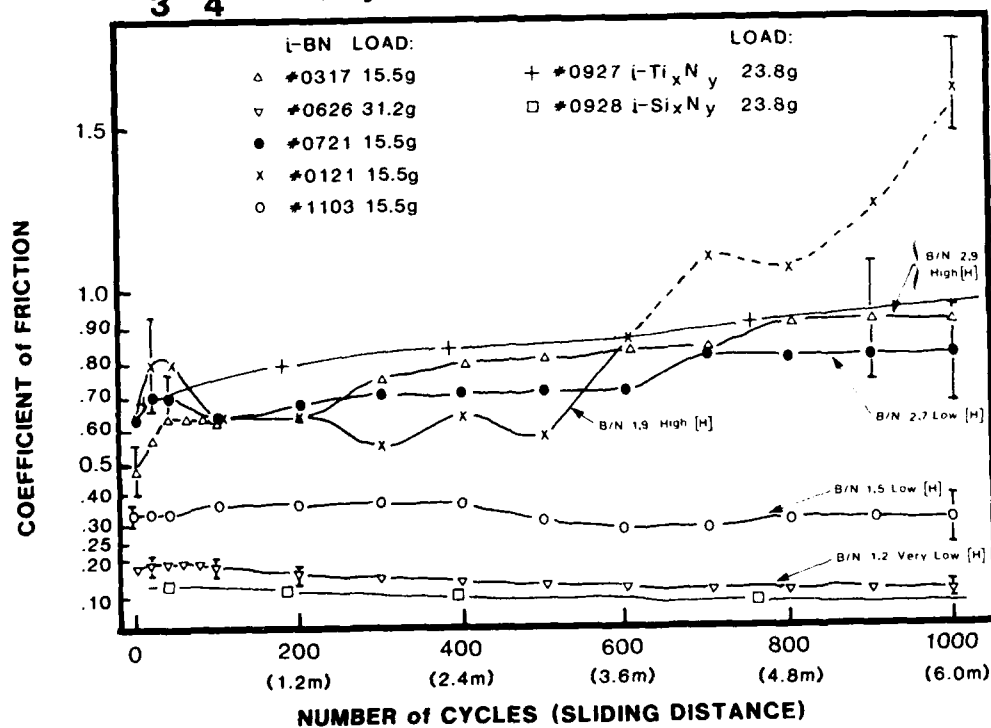


FIGURE 4-18. COEFFICIENT OF FRICTION VERSUS SLIDING DISTANCE. (Si₃N₄ ball, dry, on IBED nitride coatings.) From Reference 26.

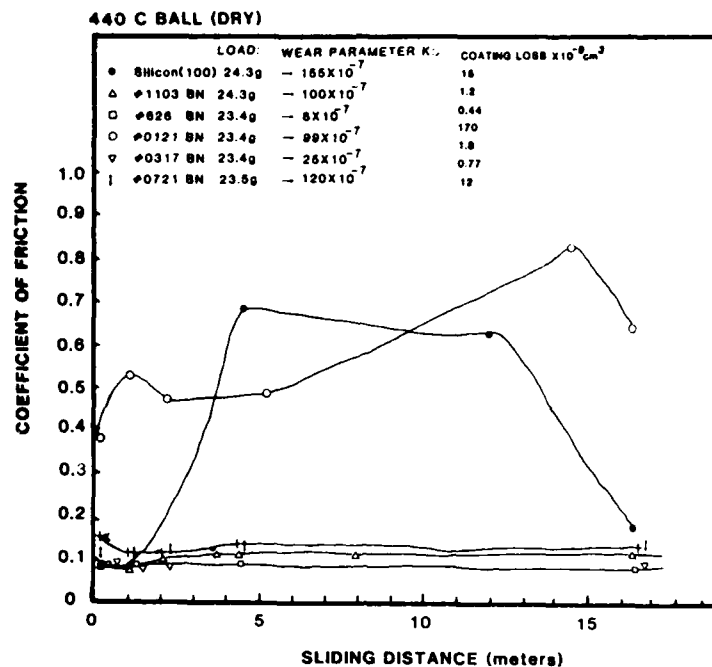


FIGURE 4-19. COEFFICIENT OF FRICTION VERSUS SLIDING DISTANCE. (440 C ball, dry, on IBED nitride coatings.) From Reference 26.

There appears to be a general increase in friction with increasing B/N ratio in the Si_3N_4 ball system while little difference is seen with the 440 C system. Hydrogen content of the film seems to have an effect on the friction in both ball systems, i.e., friction increasing with [H]. Of particular interest is coating #0121 whose friction was among the highest in both systems. Its hydrogen concentration, [H] = 12 percent, was the highest measured of all the films. It should be noted that this coating exhibited brittle behavior and that it was worn through after about 600 cycles. Data beyond this point are influenced by accumulated debris along the wear track.

In the i-BN system, adhesive transfer of ball material to the coating occurred only with sample #0317. After the 440 C ball test, several patches (~ 1000 angstroms thick) could be seen on the coating. A more continuous distribution of patches (approximately 1 micron thick) was present after the Si_3N_4 ball test. Figure 4-20 shows a SEM micrograph of this wear track. Compare this figure to Figure 4-21, which shows an SEM of the wear



FIGURE 4-20. SEM MICROGRAPH SHOWING ADHESIVE TRANSFER TO COATING #0317 FOLLOWING Si_3N_4 BALL TEST.



FIGURE 4-21. SEM MICROGRAPH OF WEAR TRACK FOR SAMPLE #0626.

track for sample #0626. Although the test for #0626 was run with twice the load and 20 times the number of cycles as sample #0317, essentially no wear was visible. Once again, this reinforces the conclusions from Figure 4-18 that a low B/N ratio and low [H] result in films with better mechanical properties in friction and wear. It should be noted that NRA of sample #0626 also indicated the presence of some carbon contamination, as mentioned earlier, and this may also contribute to the low friction/wear behavior.

In summary, we can state that many of the i-BN coatings show low friction ($\mu \sim 0.1$) against 440 C stainless steel and Si_3N_4 counterfaces. The coatings generally show a ductile behavior with very good adhesion to the Si(100) substrate. Friction seems to increase in the i-BN system with increasing B/N ratio and also when hydrogen content is higher. Hydrogen incorporation is also seen to have a deleterious effect on mechanical behavior.

SECTION 5

POSSIBLE i-BN APPLICATIONS

The advent of a relatively low temperature processes, such as IBED, for the deposition of boron nitride thin films onto a variety of substrate materials, has sparked investigation into utilizing this unique material in an ever widening variety of applications of commercial interest.

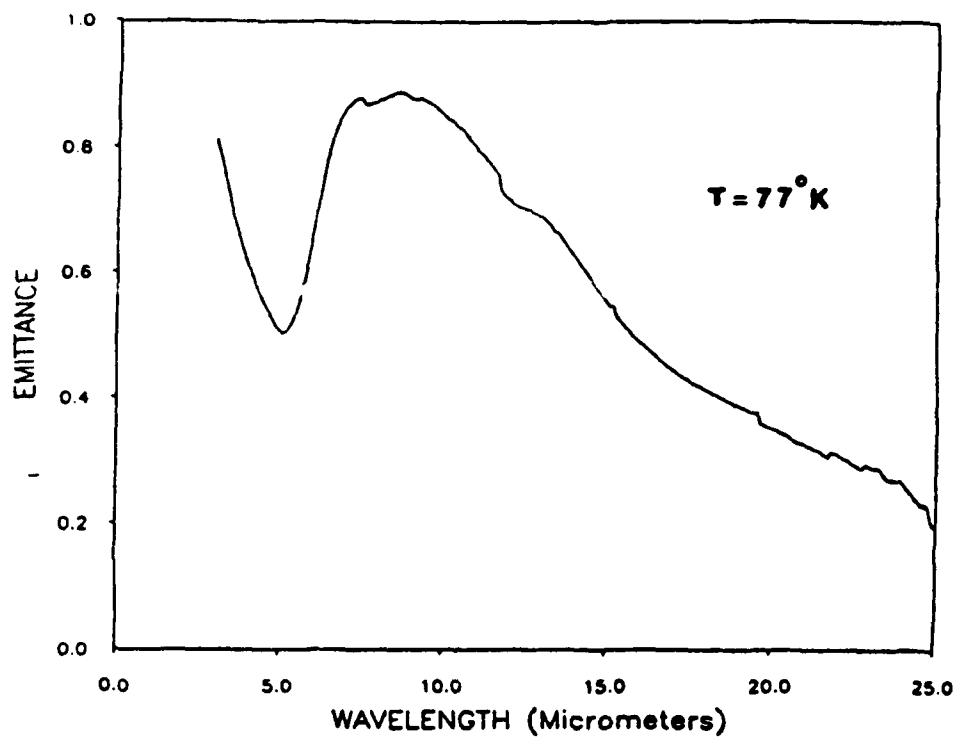
5.1 OPTICAL

Spire IBED i-BN thin films have been investigated as possible optical baffle coatings for use in telescopes. Its high spectral emittance in the 8-12 micron window (Figure 5-1) coupled with its demonstrated resistance to high energy pulsed electron radiation (Figure 5-2) has made it an interesting candidate material.

5.2 LOW-Z COATING

Research at Spire in conjunction with the DOE, MIT Fusion Center and Oak Ridge National Laboratories has been investigating using i-BN as a low-average Z ($Z=6$), refractory coating for use in plasma confinement systems. Low Z materials are preferred for use in these plasma environments because radiation losses from them produce less contamination and stability problems for the plasma. Testing at ORNL in a neutral beam test apparatus delivered 1100 pulses of 200 W/cm^2 over 2 seconds every 5 seconds. The i-BN coating survived as well as a TiC coating which is widely used now in plasma systems and has the potential advantage of having a lower Z value.

Research sponsored by both government and private sector funding has generated much promise for the eventual commercialization of i-BN thin film technology into areas which have only recently been envisioned by today's technological advances.



Full page

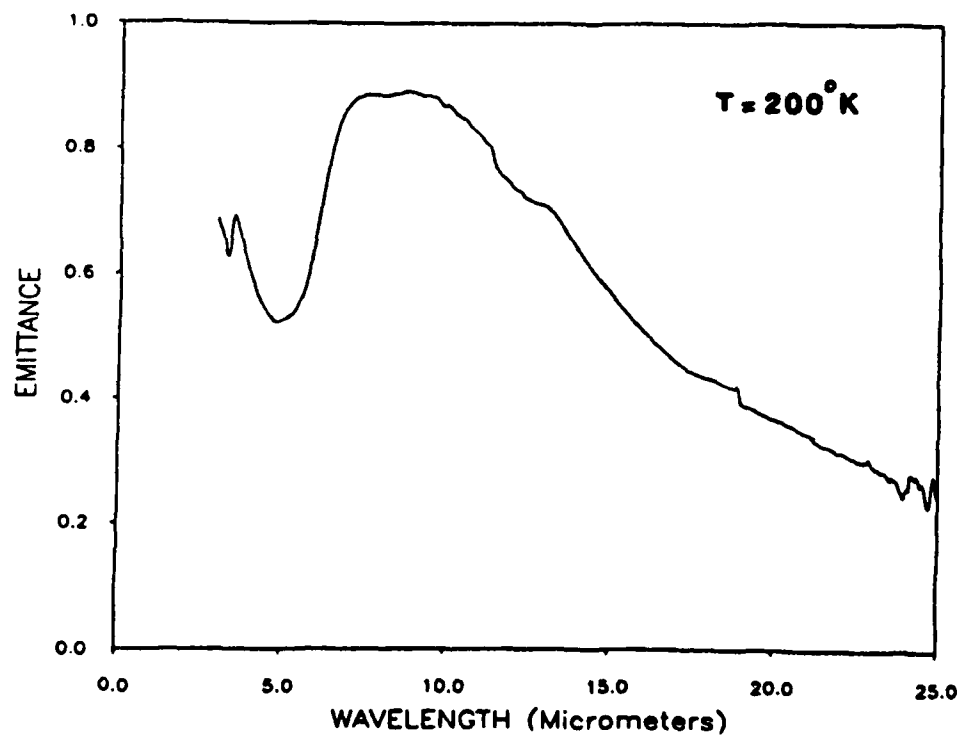


FIGURE 5-1. SPECTRAL EMITTANCE OF BORON NITRIDE ON ETCHED ALUMINUM AT 77°K AND 200°K .

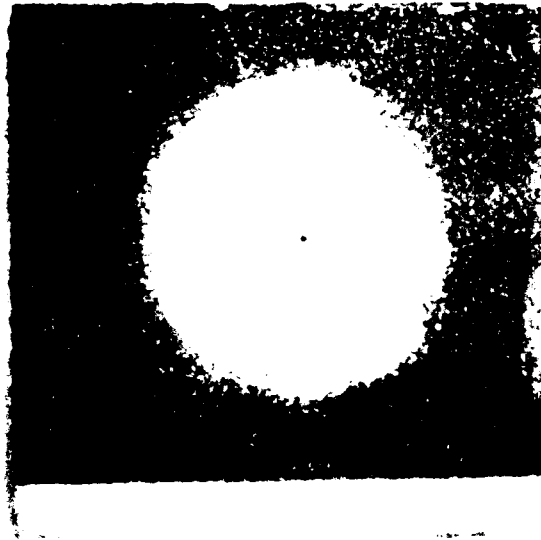


FIGURE 5-2. BLOW-OFF SCAR OF i-BN ON Al SUBSTRATE FOLLOWING PULSED ELECTRON BOMBARDMENT (3.58 cal/60 ns pulse). The outer edge of the scar where delamination was arrested received an energy flux of 0.6 cal/cm².

SECTION 6
ACKNOWLEDGEMENTS

The authors wish to gratefully acknowledge the contributions of the following individuals in providing many of the analytical results: J.P. Hirvonen, University of Helsinki (NRA, friction tests); T.C. Chou, Engelhard Corporation (XPS, RAMAN); Peter Kullen, Carnegie-Mellon (TEM); Don Potter, U. Conn. (TEM); Ray Egerton, S.U.N.Y. at Stonybrook (EELS); David Smith, Chomerics (IR).

The work presented here has been supported by the following Small Business Innovation Research (SBIR) program:

Department of Defense (Air Force)

Contract No. F33615-87-C-5203
Contract Monitor: Bob McConnell

REFERENCES

1. Harper, J.M.E.; Cuomo, J.J.; Gambino, R.J.; and Kaufman, H.R. in "Ion Bombardment Modification of Surfaces," ed. O. Auciello and R. Kelly, Elsevier Press, New York (1984).
2. Pranevicius, L.: Thin Solid Films, 1979, 63, 77.
3. Weissmantel, C.; Reisse, G.; Erler, H.J.; Henny, F.; Bewilogue, K.; Ebersvack, V.; Schurer, C.: Thin Solid Films, 1979, 63, 315.
4. Colligon, J.S.; Hill, A.E.; Kheyrandis, H.: Vacuum, 1984, 34(10/11), 843.
5. Martin, P.J.; Netterfield, R.P.; Sainty, W.G.: J. Appl. Phys., 1984, 55, 235.
6. Takagi, T.: Thin Solid Films, 1981, 92, 1.
7. Satou, M.; Andoh, Y.; Ogatag, K.; Suzuki, Y.; Matsuda, K.; Fujimonto, F.: Jap. J. of Appl. Phys., 1985, 24(6), 656.
8. Sato, T.; Ohata, K.; Asahi, N.; Ono, Y.; Oka, Y.; Hashimoto, I.: J. Vac. Sci. Tech., 1986, A4(3), 784.
9. McNeil, J.R.; Barron, A.C.; Wilson, J.R.; Herrmann, W.C.: Applied Optics, 1984, 23(4), 552.
10. Kant, R.A.; Sartwell, B.D.; Singer, I.L.; Vardiman, R.G.: See Ref. 6, 1985, 915.
11. Kennemore, C.M.; Gibson, U.J.: Appl. Optics, 1984, 23(20), 3608.
12. Martin, P.J.; Netterfield, R.P.; Sainty, W.G.: J. Appl. Phys., 1984, 55(1), 235.
13. Cuomo, J.J.; Harper, J.M.E.; Guarnieri, G.R.; Yee, D.J.; Attanasio, L.J. et al.: J. Vac. Sci. Technol., 1982, 20, 349.
14. Namba, Y. and Mori, T.: J. Vac. Sci. Technol. A, 1985, 3(2), 322.
15. Satou, M. and Fujimoto, F.: Jpn J. Appl. Phys., 1983, 22, L171.
16. Sainty, W.G.; Martin, P.J.; Netterfield, R.P.; McKenzie, D.R.; Cockayne, D.J.H.; Dwart, D.M.: J. Appl. Phys., 1988, 64(8), 3980.
17. Netterfield, R.P.; Muller, K.-H.; McKenzie, D.R.; Goonan, J.J.; Martin, P.J.: J. Appl. Phys., 1988, 63(3), 760.

18. Hubler, G.K.: J. Mat. Science & Engin., 1989 (Proceedings of the 1988 SM²IB conf.) to be published.
19. Van Vechten, D.; Hubler, G.K.; Donovan, E.P.: J. Vac. Sci. and Tech., 1988, A6, 1934.
20. Weissmantel, C.: in Thin Films From Free Atoms and Particles, ed. by K.J. Klabunde, 1985, Academic Press, NY, 153.
21. Rother, B.; Zscheile, D.; Weissmantel, C.; Heiser, C.; Holzhuter, g., Leonhardt, G.; Reich, P.: Thin Solid Films, 1986, 142, 83.
22. Hirvonen, J-P and Hirvonen, J.K.: Proceedings of Materials Research Society, 1989, 128 (to be published).
23. Feldman, L.C. and Mayer, J.W.: Fundamentals of Surface and Thin Film Analysis, 1986 (North Holland), 31.
24. Doolittle, L.R.: Nucl. Inst. Meth., 1985, B9, 344.
25. Amsel, G.; Nadai, I.P.; D'Artemare, E.; David, D.; Girard, E.; and Moulin, J.: Nucl. Inst. Meth., 1971, 92, 481.
26. Tetreault, T.G.; Hirvonen, J.K.; Parker, G.R.; and Hirvonen, J-P: Proceedings of Materials Research Society, 1989, 140 (to be published).
27. Rand, M.J. and Roberts, J.F.: J. Electrochem. Soc., 1968, 115(4), 423.
28. Satou, M.; Yamaguchi, K.; Andoh, Y.; Suzuki, Y.; Matsuda, K.; Fujimoto, F.: Nucl. Instr. and Meth., 1985, B7/8, 910.
29. Takahashi, T.; Itoh, H.; Takeuchi, A.: J. Cryst. Growth, 1979, 47, 245.
30. Chopra, K.L.; Agarwal, V.; Vankar, V.D.; Deshpandey, C.V.; Bunshah, R.F.: Thin Solid Films, 1985, 126, 307.
31. Lin, P.; Deshpandey, C.; Doerr, J.; Bunshah, R.F.; Chopra, K.L.; Vankar, V.: Thin Solid Films, 1987, 153, 487.
32. Voskoboynikov, V.V.; Gritsenko, V.A.; Effimov, V.M.; Lesnikovskaya, V.E.; Edelman, F.L.: Phys. Status Solidi (A), 1976, 34, 85.
33. Seidel, K.H.; Reichelt, K.; Schaal, W.; Dimigen, H.: Thin Solid Films, 1987, 151, 243.
34. Gielisse, P.J.; Mitra, S.S.; Plendl, J.N.; Griffis, R.D.; Mansur, L.C.; Marshall, R.; Pascoe, E.A.: Phys. Rev., 1967, 155(3), 1039.
35. Inagawa, K.; Wantabe, K.; Fanaka, I.; Saitoh, S.; Itoh, A.: Proc. 9th ISIAT Symp., Tokyo, 1985, 299.
36. Couture-Mathieu, L.; Mathieu, J-P: Comptes-Rendus Academie Des Sciences (Paris), 1953, 236, 371.

37. Ushioda, S.; Pinczuk, A.; Taylor, W.; Burstein, E.: in II-V Semiconducting Compounds, 1967, ed. D.G. Thomas, W.A. Benjamin, New York.
38. Holleck, H.: J. Vac. Sci. Technol., Nov/Dec 1986, A4(6), 2661-2669.
39. Hartley, N.E.W.: Tribology International, April 1975, 65.
40. Archard, J.F.: J. Appl. Physics, 1953, 24, 981.